HYPER-ACCRETING BLACK HOLES AND GAMMA-RAY BURSTS

Robert Popham[1], S. E. Woosley[1,2], and Chris Fryer[2]

ABSTRACT

A variety of current models for gamma-ray bursts (GRBs) suggest a common engine - a black hole of several solar masses accreting matter from a disk at a rate 0.01 to 10 $M_\odot$ s^{-1}. Using a numerical model for relativistic disk accretion, we have studied steady-state accretion at these high rates. Outside about 10^8 cm, the disk is advection dominated; energy released by dissipation is carried in by the optically thick gas and the disk does not cool. Interior to this radius, for accretion rates greater than about 0.01 $M_\odot$ s^{-1}, a global state of balanced power comes to exist between neutrino losses, chiefly pair capture on nucleons, and dissipation. As a result of these losses, the temperature is reduced, the density raised, and the disk scale height reduced compared to the advective solution. The sudden onset of neutrino losses (owing to the high temperature dependence) and photodisintegration leads to an abrupt thinning of the disk that may provide favorable geometry for jet production. The inner disk remains optically thin to neutrinos for accretion rates up to about 1 $M_\odot$ s^{-1}. Energy emitted in neutrinos is less, and in the case of low accretion rates, very much less, than the maximum efficiency factor for black hole accretion (0.057 for no rotation; 0.42 for extreme Kerr rotation) times the accretion rate, $\dot{M}c^2$. Neutrino temperatures at the last stable orbit range from 2 MeV (no rotation, slow accretion) to 13 MeV (Kerr geometry, rapid accretion) and the density from 10^9 to 10^{12} g cm^{-3}. The efficiency for producing a pair fireball along the rotational axis by neutrino annihilation is calculated and found to be highly variable and very sensitive to the accretion rate. For some of the higher accretion rates studied, it can be several per cent or more; for accretion rates less than 0.05 $M_\odot$ s^{-1}, it is essentially zero. The efficiency of the Blandford-Znajek mechanism in extracting rotational energy from the black hole is also estimated. In light of these results, the viability of various gamma-ray burst models is discussed and

[1]Max Planck Institut für Astrophysik, Garching, Germany, 85740; popham@mpa-garching.mpg.de

[2]UCO/Lick Observatory, University of California, Santa Cruz, CA 95064; woosley@ucolick.org, cfryer@ucolick.org

the sensitivity of the results to disk viscosity, black hole rotation rate, and black hole mass explored. A diverse range of GRB energies seems unavoidable and neutrino annihilation in hyper-accreting black hole systems can explain bursts up to 10^{52} erg. Larger energies may be inferred for beaming systems.

Subject headings: black holes – accretion disks – gamma-ray bursts

1. INTRODUCTION

Historically the study of black hole and neutron star accretion has been motivated by the study of active galactic nuclei and accreting (stellar mass) x-ray sources. In both cases, accretion is Eddington-limited to small rates $\dot{M} \lesssim 10^{-8}(M/\ \mathrm{M}_{\odot})\ \mathrm{yr}^{-1}$. For an interesting range of moderate accretion rates, the energy released by viscous dissipation can be radiated away efficiently and consequently the disk is thin.

For very low or very high accretion rates, however, the cooling efficiency of the disk changes and can drop to the point where most of the dissipated energy is not radiated, but carried into the hole with the accreting gas in an "advection-dominated accretion flow" (ADAF). For low accretion rates, this occurs because the radiative processes become very inefficient at low density. The dissipated energy stays in the gas, which becomes very hot, and this makes the disk geometrically thick. Recently, ADAFs corresponding to *low* accretion rates and optically thin disks have been studied in some detail (see Narayan, Mahadevan, & Quataert 1998 for a review). They have been used to model both accreting stellar-mass black holes and the supermassive black hole sources believed to lie at galactic centers.

Advection-dominated flows also occur for high accretion rates if the disk is very optically thick. Radiation does not diffuse out in a viscous time scale and so again is carried into the hole. The solutions resemble, mathematically, the ADAFs at low density since in both cases the gas cannot cool.

Eventually, however, at extremely high accretion rates, the nature of ADAFs can change again due to the onset of efficient cooling by neutrinos. For *neutron stars*, the accretion rate where neutrino losses begin to dominate photons in the energy loss budget is about $10^{-4}\ \mathrm{M}_{\odot}\ \mathrm{yr}^{-1}$ (Chevalier 1993; Fryer, Benz, & Herant 1996). For black holes, the limit is much higher because energy can disappear into the hole. As we shall see, it is only for accretion rates in excess of about 0.01 $\mathrm{M}_{\odot}$ *per second*, that neutrino radiation can cool the gas accreting into a black hole on a viscous time scale. We refer to such accretion as "neutrino dominated". The ADAF solutions one obtains neglecting neutrino emission are very different.

Besides wanting to explore new accretion physics, we are motivated by a desire to understand GRBs. Most leading models for GRBs (§2) have in common an engine based upon a "hyper-accreting black hole", a black hole of $\sim 2-10\ \mathrm{M}_\odot$ accreting mass at a rate sufficient to consume from 0.1 to several solar masses within, at most, a GRB time scale (on average 20 s for the long complex class of bursts (Fishman & Meegan 1995)).

For the steady state disks we study, the angular momentum in the initial system defines the radius where the disk forms and the viscous time scale at that radius gives the approximate duration of the event (though longer events occur if the disk is continually fed by an external source such as the collapse of a star). One conclusion of our paper will be a range of time scales and accretion rates (viscosity dependent) that should characterize various GRB models. We also calculate the variation of temperature, density, disk scale height, radial drift velocity and luminosity with radius in the disk. From these we are able to infer, albeit approximately, the efficiency for jet production based on neutrino annihilation (see also Jaroszyński 1996) as well as the energy density in the disk and the number of orbits experienced by an accreting blob. The latter has implications for whether the large magnetic fields that have been invoked for the electromagnetic acceleration of jets can accumulate (Blandford & Znajek 1977; Narayan *et al.* 1992; Hartmann & Woosley 1995; Mészáros & Rees 1997; Paczyński 1998).

Our numerical model is discussed in §3. The solutions are characterized by four physical parameters: the black hole mass, accretion rate, black hole spin parameter a, and disk viscosity parameter α. We include, in addition to the emission from pair annihilation, neutrino losses from the electron-positron pair capture on nucleons (which we find dominates the cooling), and photodisintegration. The equation of state, while simple, contains the effects of radiation, relativistic pairs, and degeneracy. Our semi-analytic solutions are thus sufficiently realistic to make qualitative predictions regarding the viability of various models for GRBs and to guide the complex multi-dimensional hydrodynamical studies that will follow (e.g., Eberl, Ruffert, & Janka 1998; MacFadyen & Woosley 1998; Fryer & Woosley 1998; Fryer et al. 1998).

We discuss the results of our calculations in §4 and describe a typical solution. We examine solutions for a variety of accretion rates, disk viscosity parameters, and black hole spin rates. For each case, we derive neutrino luminosities, which turn out to depend strongly on all of these parameters. Approximations to the accretion rate are given in §5 for various evolutionary scenarios.

In Section 6 we calculate the efficiencies of gamma-ray production by neutrino annihilation for the various models. We also estimate the efficiencies for energy extraction by the Blandford-Znajek process. The final section summarizes our conclusions and discusses the implications of our hyper-accreting black hole disk solutions for GRB models.

2. EVOLUTIONARY PATHS

There are many ways in which a black hole may come to experience rapid transient accretion. We expect that each occurs to an appreciable extent in nature; indeed given current uncertainties in such quantities as the neutron star kick velocity, common envelope evolution and the sizes of stripped helium cores during the late stages of evolution, it is uncertain just which predominates (Fryer, Woosley, & Hartmann 1998). It is likely, though, that GRBs are a diverse set of phenomena, all having at their heart a hyper-accreting black hole, but differing in accretion rate, accretion mass, rotation rate of the black hole, and surroundings (Table 1).

2.1. Merging Neutron Stars

The oldest of the binary compact object models for cosmological GRBs, merging neutron stars, were first mentioned as possible sources by Paczyński (1986) and Eichler *et al.* (1989). Progenitor double neutron star systems have long been known to exist (Hulse & Taylor 1975) and several evolutionary paths for their formation have been proposed (e.g. Srinivasan & van den Heuvel 1982; Brown 1995). For a time it was believed that the burst might originate during the merger, but this proved too inefficient (Janka & Ruffert, 1996). However, depending upon the equation of state, a result of the merger may be a black hole of about 2.5 solar masses surrounded by a disk of approximately $0.1 - 0.2$ $M_\odot$ (Ruffert & Janka 1998).

That accretion from this disk might give rise to GRBs was suggested by Narayan *et al.* (1992). The most detailed calculations to date are by Ruffert, Janka, & Schäfer (1995), Janka & Ruffert (1996), and Ruffert & Janka (1998). In particular Ruffert & Janka (1998) estimate the mass of the disk to be 0.1 - 0.2 $M_\odot$, the accretion rate about 1 $M_\odot$ s^{-1}, the neutrino luminosity about 10^{53} erg s^{-1}, the energy deposition along the polar axes by neutrino annihilation about 5×10^{50} erg s^{-1}, and thus the total energy available to make the burst about 5×10^{49} erg. Simple equations derived in §5 and efficiencies calculated in §6 agree well with these numbers.

2.2. Neutron Stars Merging With Black Holes

Paczyński (1991) and Narayan *et al.* (1992) also suggested that the merger of a neutron star with a pre-existing black hole of several solar masses might produce GRBs. In the dominant formation scenario of binaries consisting of a black hole and neutron star, the black hole is formed via hypercritical accretion during a common envelope phase (Bethe & Brown 1998). The resultant black hole has a very low mass ($\sim 3 M_{\odot}$), very similar to the double neutron star systems. Here the situation is somewhat improved because of the larger mass of the disk that forms, about 0.5 $M_{\odot}$ (Eberl 1998; Eberl, Ruffert, & Janka 1998; Kluźniak & Lee 1998) and the fact that one already has a black hole to start with. In most ways, though, this is just a more energetic analogue of the merging neutron star aftermath. Accretion rates and neutrino luminosities are higher because of the larger disk mass. The neutrino annihilation efficiency is consequently increased to a few per cent. Eberl *et al.* (1998) find disk masses of 0.5 $M_{\odot}$, accretion rates highly variable between 1 and 10 $M_{\odot}$ s^{-1}, neutrino luminosities from 10^{53} to 10^{54} erg s^{-1}, and efficiencies for neutrino annihilation of a few per cent. The total energy available for the burst is about 10^{51} erg. Depending upon beaming, this may still be inadequate to explain GRB 971214 (Ramaprakash *et al.* 1998) without invoking energy sources other than neutrino annihilation, but it may account well for the short hard bursts in the BATSE sample (Fishman & Meegan 1995). A concern both for this model and the merging neutron star model is the distance the system may travel before merging, perhaps too far to be associated with star formation. However, because the trigger threshold on Beppo-Sax exceeds a few seconds, we have no information on the optical counterparts to short GRBs.

2.3. Collapsars

The mechanism whereby the collapsing iron core of a massive star gives rise to an outgoing shock and makes a supernova remains controversial (e.g., Mezzacappa *et al.* 1997; Fryer 1998). Surely many massive stars, in their deaths, produce supernovae by forming neutron stars in spherically symmetric explosions, but perhaps not all do. Especially as the mass of the star becomes more than ~ 30 $M_{\odot}$ on the main sequence (pre-supernova helium core masses bigger than 12 $M_{\odot}$), the accretion rate of the mantle onto the proto-neutron star becomes so great, ~ 1 $M_{\odot}$ s^{-1}, and the mass of the iron core so large ($\gtrsim 2.0$ $M_{\odot}$), that a black hole may form before a neutrino powered shock is successfully launched. Woosley (1993, 1996) suggested that the outcome of such collapses would be gamma-ray bursts. This model is currently being explored in two-dimensional calculations by MacFadyen & Woosley (1998) and a very similar model, named the "hypernova", has been discussed by

Paczyński (1997). An explosion of this sort may have been associated with Supernova 1998bw (Woosley, Eastman, & Schmidt 1998).

Early on, material accretes rapidly though the poles and the angular momentum is so low that accretion through the equator is also almost unimpeded. The hole rapidly grows to over 3 $M_\odot$. But as the angular momentum of the accreting material rises to 0.5 - 1 $\times 10^{17}$ cm^2 s^{-1}, a portion of the remainder accretes through a disk. Two-dimensional calculations by MacFadyen & Woosley (1998) show that, for a 14 $M_\odot$ helium star after about 10 seconds, the polar regions are evacuated while disk accretion continues at over 0.1 $M_\odot$ s^{-1} for about 10 s (with a subsequent long, slow decline). During most of this accretion the Kerr parameter of the black hole is over 0.9.

2.4. White Dwarfs Plus Black Holes

White dwarfs may also merge with black holes at an appreciable rate (Fryer et al. 1998). Except for the smaller secondaries, formation scenarios for binaries consisting of a white dwarf and black hole parallel those of neutron stars and black holes. Fryer, Woosley, & Hartmann (1998) find that the white dwarfs formed in these binaries will preferentially have large masses ($\sim 1 M_\odot$). These massive white dwarfs are tidally disrupted at a few times 10^9 cm and form an accretion disk around the black hole. The accretion into the hole occurs by way of a disk at a rate of about $0.01 - 0.07$ $M_\odot$ s^{-1} and lasts about $10 - 70$ s. The lower accretion rate and longer timescale corresponds to low-mass white dwarfs ($M_{\rm WD} = 0.7 M_\odot$), whereas the high mass white dwarfs which dominate these binaries have higher accretion rates, but lower accretion timescales. Again the black hole is spun up by the accretion (if it were not already rotating rapidly) to spin parameters of $a \sim 0.5$.

2.5. Black Holes and Common Envelope Evolution

In many of the formation scenarios for compact binaries, a common envelope phase is required to create the short periods. The more massive component first makes a black hole or neutron star and is later enveloped as the less massive star becomes a giant. A fraction of these systems will not eject the hydrogen common envelope; instead, the rapidly accreting compact primary will merge with the secondary's helium core, accreting quickly enough to become a black hole if it is not already. The accretion of the helium core onto the black hole has been proposed as a GRB progenitor (Fryer & Woosley 1998). The helium core is disrupted by the black hole into an accretion disk with a radius equal to a fraction of the initial core, $\sim 10^9 - 10^{10}$ cm. The accretion rate, especially along the poles, can be quite large, initially perhaps 1 $M_\odot$ s^{-1}, but again the disk accretion rate is expected to be smaller (and last longer).

Detailed calculations do not exist, but the angular momentum is larger than in the collapsar model, comparable in fact to the white dwarf– black hole merger. The disk will thus form at a large radius, comparable to that of the helium core. A crude estimate is 1 - 10 $\times 10^9$ cm. At this distance the viscous time scale will range from a fraction of a minute to 10 minutes (§5; Table 1) and the accretion rate spans a comparably large range. Again the black hole may accrete an amount comparable to its mass and be spun up to high Kerr parameters.

3. COMPUTATIONAL PROCEDURE

3.1. The Physical Model

The evolutionary scenarios described above all produce rapid disk accretion ($0.01 - 10$ $M_\odot$ s^{-1}) onto a black hole of a few solar masses. For present purposes, we are interested in the gross properties of these disks rather than their detailed time-dependent behavior; so, for simplicity, we use a steady-state disk model to study this transient event. This should be a reasonable approximation, since the viscous time scales in the inner disk, which should have the highest temperature and neutrino flux, are much shorter than those in the outer disk, on which $\dot{M}$ should vary.

As discussed in §1, we expect that the disk will be unable to cool efficiently via photons, and so the energy dissipated in the disk will be advected inward. When the temperature and density are sufficiently high, neutrino cooling will become efficient. Thus our model for the disk includes advection, but also allows for cooling which varies substantially with disk radius, unlike most previous models of ADAFs. Also, because the inner regions of the disk and the spin of the black hole may be important, we solve for the structure of the disk in the Kerr metric.

Our disk model is based on the advection-dominated disk model of Gammie & Popham (1998, hereafter GP) and Popham & Gammie (1998, hereafter PG). This model solves the "slim disk" equations in Kerr geometry. The slim disk equations are a more sophisticated version of the standard thin disk equations which include radial pressure gradients and radial energy transfer. For a detailed description of these equations and the form they take in the Kerr metric, we refer the reader to GP; however, we review them here for the reader's convenience.

The units are such that $G = M = c = 1$, where M is the mass of the black hole. Later, when we present our results, we plot the variables scaled to cgs units.

The continuity equation is:

$$4\pi r\rho HV\left(\frac{\mathcal{D}}{1-V^2}\right)^{1/2} = -\dot{M}. \tag{3-1}$$

Here r is the Boyer-Lindquist radius, ρ is the rest mass density, H is the disk thickness, V is the radial velocity measured in a co-rotating frame, $\mathcal{D} \equiv 1 - 2/r + a^2/r^2$ is a relativistic correction factor, and $\dot{M}$ is the rest mass accretion rate.

The gas energy equation is

$$\rho V\left(\frac{\mathcal{D}}{1-V^2}\right)^{1/2}\left(\frac{du}{dr} - \frac{p}{\rho^2}\frac{d\rho}{dr}\right) = \Phi - \dot{q}_{tot} \equiv f\Phi \tag{3-2}$$

Here u is the internal energy, p is the pressure, Φ is the dissipation function, and $\dot{q}_{tot}$ is the total cooling rate, as described below. The parameter f measures the importance of cooling; if $f = 1$, all the dissipated energy is advected with the flow, while if $f = 0$, cooling and dissipation occur at the same rate. Most ADAF models have taken f to be constant with radius (usually $f = 1$), but here we compute f directly from the local dissipation and cooling rates. Note that if the cooling rate exceeds the dissipation rate, one can have $f < 0$.

The radial momentum equation is

$$\frac{V}{1-V^2}\frac{dV}{dr} = f_r - \frac{1}{\rho\eta}\frac{dp}{dr}, \tag{3-3}$$

where

$$f_r \equiv -\frac{1}{r^2}\frac{\mathcal{A}\gamma_\phi^2}{\mathcal{D}}(1-\frac{\Omega}{\Omega_+})(1-\frac{\Omega}{\Omega_-}). \tag{3-4}$$

The f_r term combines the effects of gravity and rotation, where $\mathcal{A} \equiv 1 + a^2/r^2 + 2a^2/r^3$ and $\gamma_\phi^2 = 1 + l^2(1-V^2)/(r^2\mathcal{A})$, $\Omega = u^\phi/u^t$ is the angular velocity, and $\Omega_\pm = \pm(r^{3/2} \pm a)^{-1}$. The radial acceleration, on the left-hand side, is given by the difference between f_r and the pressure gradient force, where η is the relativistic enthalpy $\eta \equiv (\rho + p + u)/\rho$.

The angular momentum conservation equation is

$$\dot{M}l\eta - 4\pi Hrt^r{}_\phi = \dot{M}j. \tag{3-5}$$

Here l is the specific angular momentum of the accreting gas, $j = const.$ is the angular momentum accretion rate per unit rest mass accreted. The remaining term gives the viscous angular momentum transport rate, where t^r_ϕ is the viscous stress. The expression for t^r_ϕ is rather lengthy, the calculation of it even more so, and the reader is referred to §4 of GP for a full discussion.

The equation of vertical mechanical equilibrium is

$$H^2 = \frac{p}{\rho \eta \nu_z^2}, \tag{3-6}$$

where ν_z is an effective vertical frequency. We adopt the expression derived by Abramowicz, Lanza, & Percival (1997) for ν_z:

$$\nu_z^2 = \frac{l^2 - a^2(\mathcal{E}^2 - 1)}{r^4}, \tag{3-7}$$

where $\mathcal{E} = -u_t$ is the "energy at infinity", which is conserved along geodesics.

We set the outer edge of the disk at 10^4 Schwarzschild radii, or $r = 2 \times 10^4\, GM/c^2$, and the inner edge just outside the event horizon at $r = (1 + \sqrt{1 - a^2})\, GM/c^2$, where $\mathcal{D} = 0$.

At the outer edge we impose two boundary conditions: Ω and c_s must equal their values in the self-similar advection-dominated solution of Narayan & Yi (1994). Two other conditions on the flow are provided by the requirement that the flow pass smoothly through two critical points. The first is the sonic point r_s, where $|V| \simeq c_s$. The second is the "viscous point" r_v associated with the finite propagation speed of viscous effects, where $|V| \simeq c_\nu$. Associated with each critical point are two conditions that must be satisfied for a smooth flow, as well as one degree of freedom, the location of the critical point itself.

The final boundary condition normalizes the density (the density appears in the basic equations only in the form $d \ln \rho / dr$). We now have all the boundary conditions required to solve the four first-order ordinary differential equations for V, l, ρ, and T, and to find the eigenvalue j.

One of the radial energy transfer terms included is the advection of entropy. This term can become important in situations where the cooling of the disk is very inefficient, so that the viscous time scale is shorter than the cooling time scale. This can occur when the optical thickness of the disk, as measured from the midplane to the surface, is either very low or very high. In models of advection-dominated disks, a large fraction f_{adv} of the energy dissipated in the disk is stored as entropy and advected inward with the accreting gas. GP and PG assumed that f_{adv} was constant with radius, and usually took $f_{adv} = 1$.

For the extremely high accretion rates that we are considering, the optical thickness of the disk is very large. Thus the effective temperature is much lower than the midplane temperature, and the cooling time is long, so it appears likely that the disk is advection-dominated. Highly optically thick disks where advection is important have been modeled for the case of FU Orionis objects (Popham *et al.* 1996), but even there the accretion rates ($\sim 10^{-4}$ M$_\odot$ yr^{-1}) are many orders of magnitude smaller than those considered in this paper. If radiation were the only source of cooling available, the disk would be advection-dominated; however, eventually, the disk reaches a temperature where neutrino losses become significant.

3.2. Neutrino and Photodisintegration Losses

Cooling by neutrino emission is important in regions of the disk where the temperature is sufficiently high. Because of the steep temperature and density dependence of the neutrino emissivity, we expect the onset of neutrino cooling to occur fairly abruptly at some transition radius in the disk. Outside this radius, cooling is inefficient and the disk is advection-dominated; inside, neutrinos cool the disk efficiently. Because of this, it is no longer feasible to use an f_{adv} which is constant with R.

We include two types of neutrino losses. The first is neutrino emission due to pair annihilation. These are computed from the results of Itoh *et al.* (1989,1990). A rough approximation to these results is given by the simple expression

$$\dot{q}_{\nu,\bar{\nu}} \simeq 5 \times 10^{33} T_{11}^{9} \text{ erg cm}^{-3} \text{ s}^{-1}, \tag{3-8}$$

which can be used to compare pair cooling to the other cooling terms. The second type of neutrino cooling we include is due to *capture* of pairs on nuclei. This is computed according to

$$\dot{q}_{eN} = 9.0 \times 10^{33} \rho_{10} T_{11}^{6} X_{nuc} \text{ erg cm}^{-3} \text{ s}^{-1}, \tag{3-9}$$

where $\rho_{10} = \rho/10^{10}$ g cm^{-3}, $T_{11} = T/10^{11}$ K, and X_{nuc} is the mass fraction of nucleons (Qian & Woosley 1996). To avoid confusing this pair capture loss rate with that from pair annihilation, we refer to the former as the “URCA” cooling. Note that URCA cooling will dominate when $1.8\rho_{10} > T_{11}^3$.

X_{nuc} is zero in the outer disk, but photodisintegration breaks down alpha particles into neutrons and protons once T reaches about 10^{10} K. X_{nuc} is given by

$$X_{nuc} = 30.97 \rho_{10}^{-3/4} T_{10}^{9/8} \exp(-6.096/T_{10}) \tag{3-10}$$

where this expression gives $X_{nuc} < 1$, and $X_{nuc} = 1$ elsewhere. The photodisintegration process cools the gas according to

$$\dot{q}_{phot} = 10^{29} \rho_{10} V \frac{dX}{dr} \text{ erg cm}^{-3} \text{ s}^{-1} \tag{3-11}$$

For accretion rates greater than ~ 1 M$_\odot$ s^{-1}, the disk begins to be optically thick to its own neutrino emission. We limit the actual neutrino emission to the blackbody limit (Mayle 1985):

$$L_{\nu_{\rm x}} = \frac{7}{8}\sigma_{\rm B} T^4 \tag{3-12}$$

where $\sigma_{\rm B}$ is the Stephan-Boltzmann constant. This limit corresponds to the Fermi-Dirac blackbody luminosity emitted from the neutrinosphere and is the same for each neutrino flavor ($\nu_x = \nu_e, \nu_\mu, \nu_\tau$). This estimate gives rough agreement with the results of Eberl *et al.* (1998) and allows us to extend our results to accretion rates as high as 10 M$_\odot$ s^{-1}.

3.3. Equation of State

GP and PG assumed a simple gas pressure equation of state. In the optically thin disks they were considering, radiation pressure is unimportant, and the densities are low enough that degeneracy pressure was negligible.

In the present problem, gas, radiation, and degeneracy pressure are all significant. Accordingly we write the pressure as

$$P = \rho R T \frac{(1+3X_{nuc})}{4} + \frac{11}{12} a T^4 + K\left(\frac{\rho}{\mu_e}\right)^{4/3}, \tag{3-13}$$

where R is the gas constant, $K = (2\pi hc/3)(3/8\pi m_n)^{4/3} = 1.24 \times 10^{15}$, where m_n is the nucleon mass, and μ_e is the mass per electron, which we take to be 2. The three terms represent gas pressure from nucleons, pressure from radiation and relativistic electrons and positrons, and relativistic degeneracy pressure from electrons, respectively. The corresponding expression for the internal energy is

$$u = \frac{3}{2} R T \frac{(1+3X_{nuc})}{4} + \frac{11}{4}\frac{aT^4}{\rho} + 3K\left(\frac{\rho}{\mu_e}\right)^{1/3}. \tag{3-14}$$

We have assumed that the gas is pure helium before photodisintegration, hence the factor $(1+3X_{nuc})/4$ to account for the change in gas pressure. We have compared the results of this expression to those produced by a full EOS routine by Blinnikov, Dunina-Barkovskaya, & Nadyozhin (1996), and we find that the total pressure agrees to within 10% for $10^7 \leq \rho \leq 10^{11}$, $10^9 \leq T \leq 10^{10.9}$.

4. RESULTS

Our solutions are characterized by four parameters: the black hole spin a, the viscosity parameter α, the mass accretion rate $\dot{M}$, and the black hole mass M. The values of these are determined largely by the evolutionary path which provides the mass to the disk. The black hole mass and spin depend in part on the mass and angular momentum of the progenitor star which originally collapsed to produce the black hole, but both M and a can be increased substantially by the rapid accretion we are modeling here. The mass accretion rate will depend largely on the evolutionary path which leads to the rapid accretion. The viscosity parameter α is poorly known, particularly under the kinds of temperatures and densities which are reached in these disks. Since the accretion rate is determined by the mass of the disk and the viscous time scale on which it accretes, there should be a connection between $\dot{M}$ and α, as discussed in §5.

4.1. A Typical Solution

In order to describe the general features of our solutions, we begin by focusing on a "standard model" with $a = 0$, $\alpha = 0.1$, $\dot{M} = 0.1\ \mathrm{M}_\odot\ \mathrm{s}^{-1}$, and $M = 3\ \mathrm{M}_\odot$. This model is shown in Figures 1 and 2, and repeated in some other figures for comparison purposes. In Figure 1, we compare this standard model to two other solutions. The first is a pure advection-dominated solution calculated using the same code, but with all cooling terms turned off, and including only gas pressure. This solution is identical to the one shown by GP and PG, scaled to physical units using the appropriate values of M and $\dot{M}$. The second is an analytic solution for a thin neutrino-cooled disk described in §5, which assumes Keplerian rotation, and that pair capture dominates the cooling and gas pressure dominates the pressure. Note that this analytic solution assumes a Newtonian gravitational potential. These solutions represent the two extremes of no cooling and highly efficient cooling which balances the viscous dissipation at each radius. Thus, we expect that the characteristics of our neutrino-cooled disk will fall between those of these two solutions.

At large radii, the accretion flow is simply an advection-dominated flow. Figure 1 shows that the disk is quite similar to the pure advection-dominated flow at $\log r = 9$. Densities and temperatures are too small for neutrino cooling to be significant, while optical depths are too large for significant photon cooling. The approximate surface density of the disk is $\Sigma = \rho H \sim 10^{14}$ g cm^{-2} at $r = 10^9$ cm, so the disk should be extremely optically thick to photons, but optically thin to neutrinos. Figure 2 shows that $f = 1$ at large radii, and equivalently that the cooling time scale is much longer than the accretion time scale, so the dissipated energy is advected inward before it can be radiated away. The disk is thick, with

$H \sim R$, and has substantially sub-Keplerian rotation, reflecting the importance of pressure gradients.

The first significant cooling occurs in the region from $\log r = 7.5 - 8.2$, where the nuclei photodisintegrate into nucleons. The nuclei absorb 10^{19} erg g^{-1}; this energy loss is larger than the energy added by viscous dissipation, and so the entropy of the gas decreases in this zone. This is reflected in the negative value of f in this region (Fig. 2). The disk becomes thinner, with $H \approx 10^7$ cm at $r = 10^{7.5}$ cm, and the rotation is much closer to Keplerian. Fig. 1 shows that the disk becomes more like the thin neutrino-cooled disk in this zone. Fig. 2 shows that the radiation pressure, which was the largest pressure term at $\log r = 8.2$, drops in importance as the disk becomes denser and more nucleons are produced, and gas pressure, which had dominated in the outer disk, is again the largest term at $\log r = 7.5$.

At $\log r \approx 7.5$, all of the nuclei have photodisintegrated, and the cooling due to photodisintegration shuts off rather abruptly, as shown by the sudden increase in f and in the cooling time (Fig. 2). Neutrino cooling, predominantly by pair capture, begins to become important here, but at $\log r = 7.5$ it is still well below the dissipation rate. As the gas continues to fall inward, the increasing temperature and density produce a rapid increase in the neutrino cooling rate, which gradually approaches the dissipation rate. This can be seen in the slow decrease in f from one (advection-dominated) toward zero inside $\log r = 7.5$. Radiation pressure again becomes the dominant term in the inner disk. Note that in the innermost portion of the disk, the dissipation rate briefly becomes negative where the stress and shear rate change sign due to the use of a causal viscosity prescription (see GP for more details); this produces the feature in f at $\log r = 6 - 6.4$. Near the horizon, V is approaching c and Ω drops toward $\omega \equiv 2a/(r^3 + a^2 r + 2a^2) = 0$.

The neutrino luminosity of this solution is $L_\nu = 3.35 \times 10^{51}$ erg s^{-1}, of which nearly 90% is from pair capture (see Table 2 for luminosities). This is less than 2% of $\dot{M}c^2$, a somewhat lower efficiency than the standard thin disk figure of 5.7%, due largely to the fact that much of the dissipated energy goes into the entropy of the gas and is advected into the black hole. Note that 2×10^{51} erg s^{-1} goes into photodisintegration of the nuclei. The neutrino emission from the disk comes predominantly from between $\log r \sim 6 - 7$. The disk is thin to neutrinos; $\Sigma \simeq 10^{16}$ g cm^{-2} in the inner disk, while the opacity to neutrinos is about 10^{-18} cm^2 g^{-1} giving an optical depth to neutrinos of ~ 0.01.

4.2. Solutions for Other $\dot{M}$, α, and a

Figure 3 shows solutions for $\dot{M} = 0.01, 0.1, 1, 10$ M$_\odot$ s^{-1}, all with $a = 0$, $\alpha = 0.1$, and $M = 3$ M$_\odot$. The changes in $\dot{M}$ produce substantial changes in ρ and in the neutrino luminosity, but the disk height H and radial velocity V show only small changes, and the temperature increases slowly with increasing $\dot{M}$. The density and neutrino luminosity both show a strong dependence on $\dot{M}$; this is because the increased density increases the neutrino luminosity, which makes the disk thinner and denser. The 0.01 M$_\odot$ s^{-1} solution has a very low neutrino luminosity $L_\nu \simeq 1.5 \times 10^{49}$ erg s^{-1}, while the 1 M$_\odot$ s^{-1} solution has $L_\nu \sim 8.5 \times 10^{52}$ erg s^{-1}, a factor of more than 5000 larger. At low accretion rates, the density and temperature are simply too low to permit effective cooling by neutrino emission, and nearly all the dissipated energy, apart from that lost to photodisintegration, is advected into the hole. At higher accretion rates, the high temperatures and densities allow the dissipated energy to be radiated away efficiently. In fact, both the 1 and 10 M$_\odot$ s^{-1} solutions have neutrino luminosities in excess of the dissipation rate, because the neutrino emission radiates away some of the gas entropy in addition to the dissipated energy. This can be seen in the variations in f in Fig. 3; the 0.01 M$_\odot$ s^{-1} solution has $f \simeq 1$ inside of the photodisintegration zone, while for 0.1 M$_\odot$ s^{-1} f drops gradually, reflecting the increasing fraction of the dissipated energy which is radiated away by neutrinos. The higher $\dot{M}$ solutions both quickly reach $f \lesssim 0$ in this zone, demonstrating that neutrino emission is radiating away more energy than the disk is dissipating.

Figures 4 and 5 illustrate the effects of changes in α. Each shows solutions with $\alpha = 0.1$ and 0.01; in Fig. 4 $\dot{M} = 0.1$ M$_\odot$/ s, while Fig. 5 $\dot{M} = 0.01$ M$_\odot$ s^{-1}. All have $a = 0$, $M = 3$ M$_\odot$. In both cases, decreasing α produces a solution with lower radial velocity and higher density. This results in more efficient neutrino cooling, with higher neutrino luminosities for the same $\dot{M}$. In the 0.01 M$_\odot$ s^{-1} solutions (Fig. 5), the change in α produces a dramatic change in L_ν, since the $\alpha = 0.1$ solution is very inefficient. The more efficient cooling of the $\alpha = 0.01$ solutions occurs in the inner disk, so the temperature and disk height fall below the $\alpha = 0.1$ solutions there.

One interesting feature of the $\alpha = 0.01$ solutions is that they show maxima in the density, temperature, and pressure at around $\log r = 6.6$. These are similar to the maxima seen by PG at a similar position in the disk for a solution with $\alpha = 0.001$ and a solution with $f = 0.01$. Solutions with small values for α and/or f have relatively small radial velocities outside of this radius, and build up high densities and pressures there. Inside of the pressure maxima, the gas falls in toward the hole, with large radial acceleration. This produces the drop in temperature and density, and therefore in neutrino cooling, seen in Figs. 4 and 5. This effect can also be seen, to a lesser extent, in the high-$\dot{M}$ solutions in

Fig. 3.

Figure 6 shows the effects of increasing the black hole spin a for solutions with $a = 0, 0.5, 0.95$. Changes in a have little effect at large radius. Near the hole, the high-a solutions have higher densities and stronger neutrino cooling. The horizon also moves to smaller radius as a increases. In the $a = 0.5$ solution, the neutrino luminosity due to annihilation rises dramatically from the $a = 0$ solution. This results from a small increase in temperature, since the annihilation luminosity varies approximately as T^9. It appears that here cooling due to annihilation is acting as a thermostat which prevents T from rising any further. In the $a = 0.95$ solution, most of the increase in neutrino luminosity comes from pair capture, due to the dramatic increase in density in the inner part of the disk.

Figure 7 shows solutions with $a = 0.5$ for four accretion rates: $\dot{M} = 0.01$, 0.1, 1.0, and 10 $M_\odot$ s^{-1}. This can be compared to Figure 3, where $a = 0$ solutions were shown for the same accretion rates. The $a = 0.5$ solutions have higher temperatures and densities, and produce higher neutrino luminosities. These solutions might be appropriate to the later stages of a burst event, when a substantial amount of mass and angular momentum has been added to the black hole (Figure 8).

5. APPROXIMATIONS TO THE ACCRETION RATE

For those models where the accretion rate is governed by the viscous time scale of the disk, it is possible to make a simple estimates of the accretion rate and duration of the event provided one knows the radius where the disk forms. This includes most of the models in Table 1. One must distinguish however, three classes of solutions: 1) models where the disk is being fed at a rate governed by viscous processes outside the region where neutrino losses are important - white dwarfs plus black holes and black holes plus helium stellar cores are examples; 2) models where the characteristic time scale is the viscous time scale for the disk in a region where neutrino losses approximately balance dissipation - merging neutron stars, black holes plus neutron stars, and to some extent, the collapsar model; and 3) models where the accretion rate is not governed by disk viscosity, but by other circumstances. The prime example of this last case is a collapsar where the viscous time in the disk, at least for late times and reasonable choices of α, is short compared to the free fall time of matter at a much larger radius which falls inward and feeds the disk. The general collapsar model is actually a complicated case that can lie on the boundary of all three classes.

Consider first the slowest accreting models, those of class 2. The viscous time scale is approximately $t_{visc} = r^2/\nu$, where $\nu = \alpha H^2 \Omega_K$. Thus we have $t_{visc} = \alpha^{-1}(H/r)^{-2}\Omega_K^{-1}$. For an advection-dominated disk, we have $H \sim r$, so $t_{visc} \sim \alpha^{-1}\Omega_K^{-1}$. If we assume that a mass M_{disk} deposited at a given radius r_{disk} is accreted on the viscous time scale, we can estimate the accretion rate as $\dot{M} \sim M_{disk}/t_{visc}$. In general, we find *for advective disks where neutrino losses are negligible*

$$\tau \sim 2.7\alpha^{-1}M_1^{-1/2}r_{disk,9}^{3/2} \text{ s} \tag{5-1}$$
$$\dot{M} \sim 0.37\alpha M_{disk}M_1^{1/2}r_{disk,9}^{-3/2} \text{ M}_\odot \text{ s}^{-1} \tag{5-2}$$
$$\tag{5-3}$$

Assuming the radii for disk formation - approximate values are given by just the Roche radius - one obtains the characteristics of merging white dwarf black hole pairs and black hole helium core pairs given in Table 1. These agree well with the detailed models (Fryer & Woosley 1998; Fryer et al. 1998). The accretion rate spans a large range because high mass white dwarfs (and compact helium cores) form their disks at smaller radii than those with low mass.

Next we consider neutrino dominated disks. We assume that neutrino cooling is so efficient that any energy dissipated in the disk is quickly radiated away. In other words, one assumes that neutrino cooling will produce a thin disk (Shakura & Sunyaev 1973) where advection will be unimportant. One can do this by simply substituting the neutrino cooling rate (§3) into the standard thin disk equations. There is a question of which of the two types of neutrino cooling described above will be dominant. By solving the thin disk equations for each type of cooling in turn, one can then check to see whether this should be the dominant cooling term in the resulting disk. Doing so, one finds that the thin disk should be quite dense, and, as a result, cooling by pair capture on nucleons should dominate over $\nu - \bar{\nu}$ annihilation. The thin disk solution is obtained by equating the cooling rate by pair capture to the energy dissipation rate per unit volume $(3/8\pi)\dot{M}\Omega_K^2/H$. One then finds:

$$T = 1.3 \times 10^{11}\alpha^{0.2}M_1^{-0.2}R^{-0.3} \text{ K} \tag{5-4}$$
$$H = 1.7 \times 10^4\alpha^{0.1}M_1^{0.9}R^{1.35} \text{ cm} \tag{5-5}$$
$$\rho = 1.2 \times 10^{14}\alpha^{-1.3}M_1^{-1.7}R^{-2.55}\dot{M}_1 \text{ g cm}^{-3} \tag{5-6}$$
$$V = 5.6 \times 10^8\alpha^{1.2}M_1^{-0.2}R^{0.2} \text{ cm s}^{-1} \tag{5-7}$$
$$\Omega = \Omega_K = 2.0 \times 10^5 M_1^{-1}R^{-1.5} \text{ s}^{-1} \tag{5-8}$$
$$l = 4.4 \times 10^{15}M_1R^{0.5} \text{ cm}^2 \text{ s}^{-1} \tag{5-9}$$
$$\tau = R/V = 2.6 \times 10^{-4}\alpha^{-1.2}M_1^{1.2}R^{0.8} \text{ s} \tag{5-10}$$

where M_1, R, and $\dot{M}_1$ are the mass of the accreting black hole in solar masses, the radius in gravitational radii GM_1/c^2 (4.43 km for a 3 $M_\odot$ black hole), and the mass accretion rate in solar masses per second. Note that the pair capture rate is proportional to X_{nuc}, which is taken to be unity. These equations then provide the estimates given in Table 1 for the merging neutron stars and neutron star black hole pairs. Again, for an assumed disk viscosity $\alpha = 0.1$ and black hole mass, $M_1 = 3$ $M_\odot$, they are not far from the detailed models (Ruffert & Janka 1998; Eberl, Ruffert, & Janka 1998) provided a disk radius of 50 km is adopted. This solution is shown in Fig. 1 for comparison with our calculations.

Finally we consider the collapsar. The angular momentum distribution inside a collapsing massive stellar core is unknown. Such calculations as have been done (Heger, Woosley, & Langer 1998) indicate an increasing value for l as one moves out in mass, rising from a few $\times$ 10^{16} cm^2 s^{-1} in the inner few solar masses to about 10^{17} cm^2 s^{-1} in the outer regions. One expects considerable variations from star to star. This range of l corresponds to disk radii of 50 - 250 km and viscous time scales (neutrino dominated) of about 0.1 s. However, this is considerably shorter than the free fall time for the mass that feeds the disk. For a stellar radius that contains most of the mass of, e.g., a 10 $M_\odot$ helium core, $\sim 5 \times 10^9$ cm, the free fall time scale 1338 s$/\rho^{1/2}$ is several seconds, and this time scale grows longer as the accretion continues. The collapsar is probably unable to produce a jet during its first 5 - 10 s because the infalling matter along the rotational axis sweeps any energy deposited into the hole. So a time scale of $\sim$ 10 s seems reasonable for the collapsar. This is consistent with detailed 2D models (MacFadyen & Woosley 1998).

6. ENERGY CONVERSION EFFICIENCIES

According to the current paradigm (Rees & Mészáros 1992, 1994, and subsequent publications; Katz 1994; Sari & Piran 1997a,b), a gamma-ray burst is formed when a relativistic outflow, most likely a jet, suffers collisions both internally and with the surrounding medium, producing shocks. Typical values needed for the jet are relativistic Γ's of $\gtrsim 100$. The total mass and energy of the jet depends upon its opening angle and the efficiency for converting its energy to gamma-rays, but should be of order $10^{-6} - 10^{-5}$ $M_\odot$ and $10^{50} - 10^{51}$ erg. Modern gamma-ray burst models thus divide into two categories: those that treat the shock interaction and production of gamma-rays and "afterglows" in other wavelengths (e.g., Waxman 1997) and those that discuss the energy source itself. We are interested here only in the latter problem.

The main problem in all current models for the GRB energy source is how to convert some fraction (albeit small) of the net accretion energy into directed relativistic outflow. Two general mechanisms have been proposed - neutrino annihilation and magnetohydrodynamical (MHD) mechanisms of various kinds. The former is easier to understand and to model and will be dealt with first.

6.1. Efficiency for neutrino annihilation

Table 2 shows that a highly variable fraction of the accretion energy will be emitted as neutrinos. In general a higher accretion rate and a low viscosity favor high efficiencies, $L_\nu/\dot{M}c^2$. A large rotation rate for the black hole also enhances the efficiency. Most of these neutrinos come from pair capture on nucleons and are thus solely of the electron flavor. The smaller fraction of neutrinos from pair annihilation will be a mixture of three flavors. Everywhere in the vicinity of the black hole, but especially along the rotational axis, neutrino will encounter neutrino with a large flux. Thus neutrino annihilation, $\nu + \bar{\nu} \rightarrow e^+ + e^-$, will deposit some fraction of the accretion energy in regions where the mass density may be small. These same neutrinos will also drive a wind from the disk by their interaction with electrons and nucleons. Since the gravitational potential, neutrino temperatures, and fluxes are similar to those for neutron stars, the semi-analytic formulae of Qian & Woosley (1996) should hold approximately. This suggests that the wind from the disk will be negligible except in the case of neutron star–black hole mergers. There it might amount to ~ 0.01 M$_\odot$ s^{-1}.

We neglect here the interaction of neutrinos with all other matter and estimate the neutrino annihilation efficiency using a simple approximation to the disk geometry. The neutrino luminosity is assumed to be concentrated in the equatorial plane (a good approximation given the high temperature sensitivity of the rates) and thus to have a luminosity $4\pi r H(r)\dot{q}(r)$ erg cm^{-1} s^{-1} where $H(r)$ is the disk scale height and $\dot{q}(r)$ the neutrino luminosity per unit volume evaluated for the temperature and density at radius r. The neutrino annihilation at any point above the disk is calculated following the method described in Ruffert *et al.* (1997):

$$\begin{aligned} l^+_{\nu\bar{\nu}}(\nu_i\bar{\nu}_i) = A_1 \sum_k \frac{\Delta L^k_{\nu_i}}{d_k^2} \sum_{k'} \frac{\Delta L^{k'}_{\nu_i}}{d_{k'}^2} [\langle\epsilon\rangle_{\nu_i} + \langle\epsilon\rangle_{\bar{\nu}_i}](1-cos\theta)^2 \\ + A_2 \sum_k \frac{\Delta L^k_{\nu_i}}{d_k^2} \sum_{k'} \frac{\Delta L^{k'}_{\nu_i}}{d_{k'}^2} \frac{\langle\epsilon\rangle_{\nu_i} + \langle\epsilon\rangle_{\bar{\nu}_i}}{\langle\epsilon\rangle_{\nu_i}\langle\epsilon\rangle_{\bar{\nu}_i}}(1-cos\theta) \end{aligned} \tag{6-1}$$

where $A_1 = \sigma_0(C_1 + C_2)_{\nu_i\bar{\nu}_i}/(12\pi^2 c^5 m_e^2) \approx 1.7 \times 10^{-44}\,\mathrm{cm\,erg^{-2}\,s^{-1}}$ and $A_2 = \sigma_0(C_3)_{\nu_i\bar{\nu}_i}/(4\pi^2 c) \approx 1.6 \times 10^{-56}\,\mathrm{cm\,s^{-1}}$ are the neutrino cross-section constants for electron neutrinos (including geometrical factors). We model the disk as a grid of cells in the plane with neutrino mean energy ($\langle\epsilon\rangle_{\nu_i}$) and luminosity ($\Delta L^k_{\nu_i}$). For each pair of cells, and every point above the scale height of the disk $H(r)$, we calculate distance (d_k)

from each cell to that point, and the angle (θ) at which the neutrinos and anti-neutrinos from the pair of cells interact. The summation over all pairs of cells gives the energy density from pair production at that point.

Each of the neutrino energies and luminosities includes the effects of general relativity as the neutrinos travel through the black hole's potential well. Those neutrinos which annihilate near the surface of the black hole were emitted further out in the potential well and actually gain energy before annihilation. However, the pairs they produce must then climb further out of the potential well, an effect that almost exactly cancels out the energy gain. In addition, most of the annihilation energy is produced well above the black hole and general relativity plays a very minor role (<5%) in the total fireball energy. We have not modeled neutrino propagation through a Kerr metric, nor have we modeled the bending of geodesics, but it is unlikely that these effects will significantly alter our results.

For our models, most of the neutrino emission is due to electron capture and the luminosity density from pair production ($l^+_{\nu\bar{\nu}}(\nu_i\bar{\nu_i})$) is dominated by the annihilation of electron neutrinos and anti-neutrinos. Although we include the contribution of the μ and τ neutrinos for completeness, they make up less than 10% of the total luminosity density.

Integrating over the distance above the plane and taking advantage of the cylindrical symmetry of our disk:

$$2\pi r \int_0^\infty l^+_{\nu\bar{\nu}}(\nu_i\bar{\nu_i})dz \tag{6-2}$$

demonstrates the strong focusing of the pair fireball (Fig. 9) For most of the models, over half of the energy is injected at equatorial radii $\lesssim 2 \times 10^6$ cm. Further integrating the luminosity over the equatorial radius gives the total neutrino annihilation luminosities. The net momentum of the pairs produced by this annihilation is directed *outward* along the angular momentum axis, and most of this energy will escape. Table 4 summarizes the neutrino annihilation energies and efficiencies for all models studied. The efficiency of energy conversion from neutrinos to a electron/positron pair fireball is both a function of the total neutrino emission and the distribution of that emission. For example, although the $\dot{M} = 0.1$ M$_\odot$ s^{-1}, $\alpha = 0.1, a = 0$ model has a lower luminosity than its $\alpha = 0.01$ counterpart, because its emission is more centrally concentrated, it converts a larger fraction of the neutrinos into electron/positron pairs and its resultant fireball is more energetic.

Note that the energy conversion efficiencies are extremely high for the $\dot{M} = 10$ M$_\odot$ s^{-1} models. For these models, our assumption that the disk is optically thin to neutrinos no longer holds (the neutrino mean free path is $\sim 1000 - 5000$ cm whereas the disk scale height is 10^5 cm). For the non-rotating model, our estimated luminosity exceeds that of Eberl, Ruffert, & Janka (1998) by nearly a factor of 4. Most of this factor arises from the fact that our models predict that nearly all of the neutrino energy is produced by electron capture (increasing our efficiency by a factor of 3), and hence, is dominated by electron neutrinos and anti-neutrinos. Although we have limited our neutrino luminosity by the blackbody limit, overestimates in the neutrino temperature no doubt account for the remaining 30-40% differences. Our estimates for the $\dot{M} = 10$ $M_\odot$ s^{-1} models should be taken as an upper limit for the neutrino annihilation luminosity, and the actual luminosity could be as much as a factor of 5 lower.

6.2. Blandford-Znajek efficiencies

It is also possible to extract energy from either the disk or the black hole by MHD processes (e.g., Narayan *et al.* 1992; Mészáros & Rees 1997). Perhaps the easiest of these to estimate is the Blandford-Znajek (1977, BZ) efficiency for extracting rotational energy from the black hole. This does not mean that other MHD processes – e.g., Parker instability in the disk (Narayan *et al.* 1992) – are negligible, but we give here the BZ–efficiency as a rough estimate.

All the mechanisms in Table 1 give black holes which are rotating very fast. This is inherent in the fact that they accrete a fraction of their mass from a disk. Typical values of the spin parameter a are 0.5 and we adopt that here as a representative value. The magnetic field in the accreting plasma is harder to estimate. Here we follow a common assumption that the field will rise to some fraction, which we guess might be 10% of its equipartition value (i.e., an energy density 1% of ρv^2). Table 3 gives values of ρv^2; typical values are 10^{30} erg cm^{-3} implying a field strength of $10^{14} - 10^{15}$ gauss. The BZ jet luminosity is then

$$L_{\rm BZ} \approx 10^{50}\, a^2 \left(\frac{B}{10^{15}\rm gauss}\right)^2 \quad {\rm erg\ s^{-1}} \tag{6-3}$$

Entries for our various models are given in Table 6.

Note that to generate the equipartition field requires not only a large kinetic energy density in the vicinity of the of the black hole but that the disk make many revolutions. Table 3 gives the number of windings a blob of accreting matter will experience in each of our models. The number required to generate the field depends upon the primordial field in the accreting matter and the efficiency of instabilities in creating radial variations in a magnetic field whose poloidal component is being wound by rotation. We suspect that 10 windings is a gross lower bound.

7. CONCLUSIONS AND IMPLICATIONS FOR GAMMA-RAY BURSTS

We have explored accretion at very high rates, 0.01 to 10 $M_\odot$ s^{-1} into stellar mass black holes. The black holes were of both the stationary (Schwarzschild) and rapidly rotating (Kerr) varieties. For a disk viscosity $\alpha = 0.1$ and accretion rates larger than ~ 0.05 $M_\odot$ s^{-1}, we find that a situation of global balanced power comes to exist in the disk interior to about 10^8 cm where neutrino emission, chiefly by pair capture on nucleons, approximately balances the energy dissipated by viscosity (Table 2). For lower disk viscosity, the necessary accretion rate to achieve balanced power is reduced (see $\alpha = 0.01$, $\dot{M} = 0.01$ $M_\odot$ s^{-1}, Table 2). Loss of appreciable energy to neutrinos leads to a cooler, denser, and thinner disk than the purely advective solution (Fig. 1). The sudden onset of neutrino losses, which are very sensitive to the temperature and density, appreciably thins the disk and may help to provide favorable geometry for jet acceleration.

Temperatures in the inner disk range from 2 MeV to 13 MeV in the models studied and densities from 10^9 to 10^{12} g cm^{-3} (Table 3). Only for the most extreme accretion rates, $\dot{M} \gtrsim 1$ $M_\odot$ s^{-1}, does the disk start to become optically thick or the neutrino emission blackbody limited. Thus one can calculate the neutrino losses and the efficiency for neutrino annihilation using a very simple approach.

We found that the efficiency for converting accreted mass energy, $\dot{M}c^2$, into neutrinos is highly variable. Greater efficiency is favored by low viscosity and high accretion rate, but in no case is the full theoretical limit reached. In some cases the efficiency is very low (e.g., 0.08% for $\alpha = 0.1$ and $\dot{M} = 0.01$ $M_\odot$ s^{-1}. The efficiency is also smaller if the black hole mass is larger (Table 2).

We also calculated the efficiency for neutrino annihilation for all of our models and found a very large range (Table 4). This range is a consequence of the large fraction of accretion energy advected into the hole for accretion rates under 0.05 $M_\odot$ s^{-1}, which reduces the neutrino luminosity, and a reduction in mean neutrino energy for the cooler, slower accreting disks, which reduces the cross section for neutrino annihilation. For a Schwarzschild black hole, changing the accretion rate by one order of magnitude from 0.01 $M_\odot$ s^{-1} to 0.1 $M_\odot$ s^{-1} changes the energy deposition by neutrino annihilation by five orders of magnitude. Above 0.1 $M_\odot$ s^{-1} the efficiency for neutrino annihilation continues to increase reaching at least several per cent for accretion rates of 5 $M_\odot$ s^{-1} on a rapidly rotating black hole. It is impossible to produce a bright GRB (of say 10^{49} ergs which, with a beaming factor of 100, might resemble a 10^{51} erg burst) by neutrino annihilation in any model in which the accretion rate is less than a few $\times 10^{-2}$ $M_\odot$ s^{-1}. On the other hand accretion rates over 0.1 $M_\odot$ s^{-1}, however they may be realized, can give very energetic events (Tables 4 and 5).

With the energy densities calculated for our inner disks we also estimate the efficiency for jet acceleration by the Blandford-Znajek (BZ) process using a representative value for the spin parameter (0.5) and a guess regarding the the magnetic energy density (1% of ρv^2 in the inner disk). Typical total GRB energies were around 10^{50} erg (times the beaming factor). These estimates are very crude; in particular, the field energy density in the disk could be 1%, 100%, or 0% of equipartition. We give these estimates only to show that the kinetic energy density in the disk is sufficient to anchor an adequate field to power a bright (beamed) GRB.

However, we note that these large fields might require many orbits of the disk to generate. The number of disk windings is small unless the viscosity is initially low (Table 3). One can envision a disk that has essentially zero viscosity until the field is wound up to a significant fraction of equipartition. Then the estimates of field strength in the inner disk (Table 6) would be higher. We see two solutions to the GRB problem emerging - high viscosity disks that make bursts by neutrino annihilation, and low viscosity disks that extract rotational energy from the black hole by MHD processes. Our understanding of the disk physics is inadequate to distinguish these at the present time. We have concentrated on neutrino annihilation here simply because it is easier to calculate.

The implications of our work for GRB models are best discussed on a case by case basis (see Tables 5 and 6). The event rates in Table 5 are representative and are taken from the forthcoming paper by Fryer, Woosley, & Hartmann (1998).

7.1. Merging Neutron Stars and Black Hole Neutron Star Pairs

Our calculations here qualitatively confirm the more accurate, but specialized work of Ruffert & Janka (1998) and Eberl, Ruffert, & Janka (1998). Given that a disk forms at $\sim$50 km, eq. 5.9 gives the correct approximate accretion time scale, 0.1 s, provided $\alpha = 0.1$ and the black hole mass is 3 $M_\odot$. For other values of α and black hole mass, our results suggest how their results might be scaled. Our neutrino luminosity, about 10^{53} erg s^{-1}, neutrino annihilation rate, 5×10^{50} erg s^{-1}, and total energy available for the burst, 5×10^{49} erg, agree with the detailed calculations of merging neutron stars.

For neutron star plus black hole mergers, our calculations suffer from the disk becoming optically thick. The time scale for accretion, still 0.1 s, agrees well, and for the larger disk mass (Table 1), it is clear that greater energies and efficiencies will be developed. The entries in Table 5 come from logarithmic interpolation in Table 4 to obtain the neutrino annihilation luminosity for an accretion rate of 5 $M_\odot$ s^{-1}, then arbitrary division by 4 to correct for the decrease in neutrino luminosity and cooling of neutrino energy one expects for a (optically) thick disk. These numbers are then consistent with Eberl, Ruffert, & Janka (1998).

The chief new result of our calculations here is an estimate of the effect of using Kerr geometry. The 3D numerical calculations of Eberl, Ruffert & Janka (1998) were all carried out for a non-rotating black hole. Here we see that a Kerr parameter of only 0.5 increases the efficiency of neutrino (emission and) annihilation by a factor of 4 to 6. This degree of rotation is reasonable for a black hole made by merging neutron stars, and, depending on its formation process, might be reasonable for a black hole merging with a neutron star.

Of all the models in Table 5, only the merging neutron stars and black hole–neutron star pairs have a characteristic time scale much less than one second. They are thus the only model capable of explaining the abundant subclass of short (average duration 0.3 s) hard GRBs (Fishman & Meegan 1995). We have no information on the optical counterparts of these short bursts, and do not know if they are associated with star formation.

Because the initial conditions are so uniform, especially for merging neutron stars, one might expect that the jet has a nearly unique energy and duration. GRB diversity in this case would solely reflect the variable characteristics of the interstellar medium in which the burst was embedded.

7.2. Collapsars

Here our results are more sensitive to uncertain parameters and a diversity of outcomes is possible. In addition to the uncertain disk viscosity which plagues all accretion powered models, the accretion rate is particularly sensitive to the angular momentum distribution of the accreting star. This is poorly known and likely to be highly variable both within a star and from star to star. The radius where the disk forms varies as l^2 (eq. 5.8) and the accretion rate as an even higher power. Fortunately, if the disk viscosity is adequately high, and if a steady state disk forms, the accretion rate may be determined by simpler physics – the rate at which matter is delivered to the accretion disk by the collapsing star. Our estimate comes from taking the free fall time of the star divided into that fraction of the star's mass which forms a bound disk. We estimate 10 s for the former and perhaps a few solar masses for the latter. The frequency of events is also very uncertain. In Table 5 we have taken from 0.5% to 5% of the supernova rate.

The formation of a bound disk requires dissipation. The disk of a collapsar may be unique in nature in that it is assembled from optically thick matter falling in, essentially freely from infinity. In the absence of neutrino losses and photodisintegration (which only occur inside a few hundred km), the net binding energy of the disk must be carried away by outflowing matter. This can be a considerable amount of energy. For example, a 1 $M_\odot$ disk forming at 250km ($l \simeq 10^{17}$ cm^2 s^{-1}) must release a binding energy of 3×10^{52} erg. Half of this is rotational energy and most of the rest is internal energy. But if even a small fraction goes into outflows, they could power an energetic supernova like SN 1998bw (Woosley, Eastman, & Schmidt 1998). Because a lot of the matter that flows out will have been at small radii and very hot, its composition may be rich in ^{56}Ni. Our simple steady state calculations here cannot model the multi-dimensional physics of disk formation and bi-directional flow. Two dimensional studies are in progress (MacFadyen & Woosley 1998).

But provided enough dissipation occurs, by mass ejection, viscous interaction, photodisintegration, and neutrino losses, something resembling a steady state accretion disk will form. As the accretion proceeds the black hole will be spun up. Our results show (Table 4) that the energy available for jet production from neutrino annihilation is highly variable ranging from essentially zero, if the accretion rate is 0.01 $M_\odot$ s^{-1} or less, to over 10^{52} erg if the black hole rotates rapidly and the accretion rate exceeds 0.1 $M_\odot$ s^{-1} for 10 s (Table 5). This makes collapsars potentially the most energetic and most frequent of all GRB models. If the beaming factor is $\sim$100, as preliminary calculations by MacFadyen & Woosley (1998) indicate, GRBs of equivalent energy up to 10^{54} erg might be explained.

It should be noted that in this and all models with long time scales, the energy available for a GRB is the GRB duration times the jet luminosity - not necessarily the total energies in Tables 5 and 6. This is another reason why only merging neutron stars and black holes can make energetic GRBs shorter than 1 s.

7.3. White Dwarfs Plus Black Holes

For these models the accretion rate is expected to be lower. The Roche radius gives a range of disk sizes and, for a given disk viscosity and white dwarf mass, this sets the range of accretion rate (Table 1). For the lower values, the energy from neutrino annihilation is negligible. For the higher mass white dwarfs which give accretion rates of 0.07 $M_\odot$ s^{-1} for 15 s, the energy is dramatically greater. If the black hole rotates, the yield is further increased to perhaps 10^{50} erg. We expect the beaming factor to be less here than in the collapsar, but bursts of up to 10^{51} erg might be explained, more if the Blandford-Znajek mechanism is effective (Table 6). However, unless these events occur more frequently than black hole–neutron star mergers, they are not likely to be the leading cause of GRBs.

7.4. Black Holes and Common Envelope Evolution

As with the collapsar which it resembles, this is a model where critical parameters remain poorly determined. The three dimensional evolution of a black hole merging with a helium core (or helium star) of comparable or greater mass has not been studied. One expects a great deal of the accretion to occur along the poles. The radius at which the helium disk forms is poorly known. *If* it is as small as 10^4 km for at least 1 $M_\odot$ of helium, accretion rates of 0.1 $M_\odot$ s^{-1} may be realized. If the black hole further has a Kerr parameter of 0.5, the neutrino annihilation energy would be $\sim 10^{51}$ erg. If the rotation of the black hole becomes even faster as a consequence of the merger, the energy could be increased still more. Because of the large mass and angular momentum in the merger, the channeling of the jet may result in tighter beaming, comparable to the collapsar and more focused than merging compact objects.

This research has been supported by a cooperative grant between the MPA, Garching, and UCSC from the NSF and DAAD (NSF INT 9726315 and DAAD 315) and at UCSC by NASA (NAG5-2843 and MIT SC A292701), and the NSF (AST-97-31569). We acknowledge many helpful conversations on the subject of gamma-ray bursts with Andrew MacFadyen, Alex Heger, Max Ruffert, Thomas Janka, and Eli Waxman, and thank Peter Mészáros, Bohdan Paczyński, and Martin Rees for useful comments.

REFERENCES

Abramowicz, M. A., Lanza, A., & Percival, M. J. 1997, ApJ, 479, 179

Bethe, H. A., & Brown, G. 1998, ApJ, in press

Blandford, R. D., & Znajek, R. L. 1977, MNRAS, 179, 433

Blinnikov, S. I., Dunina-Barkovskaya, N. V., & Nadyozhin, D. K. 1996, ApJS, 106, 171

Brown, G. E. 1995, ApJ, 440, 270

Chevalier, R. A. 1993, ApJ, 411, L33

Eichler, D., Livio, M., Piran, T., & Schramm, D. N. 1989, Nature, 340, 126

Eberl, T. 1998, Diploma thesis, Technische Universität München

Eberl, T., Ruffert, M., & Janka, H.-Th. 1998, A&A, in preparation

Fishman, G. J., & Meegan, C. A. 1995, ARAA, 33, 415

Fryer, C. L., Benz, W., & Herant, M. 1996, ApJ, 460, 801

Fryer, C. L., & Woosley, S. E. 1998, ApJ, in press

Fryer, C. L., Woosley, S. E., Herant, M., & Davies, M. 1998, ApJ, in preparation

Fryer, C. L., 1998, proceedings of the 2nd International Workshop on Laboratory Astrophysics with Intense Lasers, to appear in ApJ supplements, ed. Remington

Fryer, C., Woosley, S. E., & Hartmann, D. H. 1998, ApJ, in preparation

Gammie, C., & Popham, R. 1998, ApJ, 498, 313 (GP)

Hartmann, D. H., & Woosley, S. E. 1995, Advances in Space Research, 15(5), 143

Heger, A., Woosley, S. E., & Langer 1998, ApJ, in preparation

Hulse, R. A., & Taylor, J. H. 1975, ApJ, 201, L55

Itoh, N., Adachi, T., Nakagawa, M., Kohyama, Y., & Munakata, H. 1989, ApJ, 339, 354

Itoh, N., Adachi, T., Nakagawa, M., Kohyama, Y., & Munakata, H. 1990, ApJ, 360, 741

Janka, H.-Th., & Ruffert, M. 1996, A&A, 307, L33

Jaroszyński, M., 1996, A&A, 305, 839

Katz, J. 1994, ApJ, 422, 248

Kluźniak, W., & Lee, W. H., 1998, ApJ, 494, L53

MacFadyen, A., & Woosley, S. E. 1998, ApJ, in preparation

Mayle, R. W., 1985, Ph.D. Thesis, LLNL preprint UCRL-53713

Mészáros, P., & Rees, M. J. 1992, MNRAS, 257, P29

Mészáros, P., & Rees, M. J. 1997, ApJ, 482, L29

Mezzacappa, A., Calder, A. C., Bruenn, S. W., Blondin, J. M., Guidry, M. W., Strayer, M. R., & Umar, A. S. 1998, ApJ, 495, 911

Narayan, R., Mahadevan, R., & Quataert, E. 1998, to appear in "The Theory of Black Hole Accretion Discs", eds. M. A. Abramowicz, G. Bjornsson, and J. E. Pringle (astro-ph/9803141)

Narayan, R., Paczyński, B., & Piran, T. 1992, ApJ, 395, L83

Narayan, R. & Yi, I. 1994, ApJ, 428, L13

Paczyński, B. 1986, ApJ, 308, L43

Paczyński, B. 1991, Acta Astron., 41, 257

Paczyński, B. 1998, ApJ, 494, L45

Popham, R., & Gammie, C. 1998, ApJ, in press

Popham, R., Kenyon, S., Hartmann, L., & Narayan, R. 1996, ApJ, 473, 422

Qian, Y. Z., & Woosley, S. E. 1996, ApJ, 471, 331

Pringle, J. E. 1981, ARA&A, 19, 137

Ramaprakash, A. N., *et al.* 1998, Nature, 393, 43

Rees, M. J., & Meszaros, P. 1992, MNRAS, 258, 41P

Rees, M. J., & Meszaros, P. 1994, ApJ, 430, L93

Ruffert, M., Janka, H.-T., Takahashi, K., Schaefer, G. 1997, A&A, 319, 122

Ruffert, M., Janka, H.-Th., & Schäfer, G. 1996, A&A, 311, 532

Ruffert, M., & Janka, H.-Th. 1998, A&A, in preparation

Sari, R., & Piran, T. 1997, ApJ, 485, 270

Sari, R., & Piran, T. 1997, MNRAS, 287, 110

Shakura, N. I. & Sunyaev, R. A. 1973, A&A, 24, 337

Srinivasan, G., & van den Heuvel, E. P. J. 1982, A&A, 108, 143

Waxman, E. 1997 ApJ, 489, L33

Woosley, S. E., 1993, ApJ, 405, 273

Woosley, S. E. 1996, in *Gamma-Ray Bursts: 3rd Huntsville Symposium*, AIP Conf. Proc 384, eds. C. Kouveliotous, M. Briggs, & G. Fishman, AIP:New York, 709

Woosley, S. E., Eastman, R. G., & Schmidt, B. 1998, ApJ, submitted

TABLE 1

Model	$M_{accrete}$ ($M_\odot$ [a])	Radius (km)	$\dot{M}$ ($M_\odot$/s)	j (10^{16} cm^2 s^{-1})	Duration (sec)	Gravity Waves
n*+n*	0.1	50	1	4	0.1	Yes
n*+BH	0.5	50	5	4	0.1	Yes
Collapsar	2	50 - 250	0.1	5 - 10	10-20	No
BH+WD	1	(1-5)$\times 10^4$	0.01 - 0.07	50 - 150	15 - 150	No
BH+He core	2	(1- 10)$\times 10^4$	0.01 - 0.1	50 - 200	15 - 500	No

[a] Masses are for accretion through a disk. The total accretion rate, e.g. in the collapsar and He core models, is greater because of mass infall along the poles. The assumed mass of the black hole is 3 $M_\odot$ in all cases and the disk viscosity, $\alpha = 0.1$.

TABLE 2

Model				Luminosities (10^{51} erg/ s)						
$\dot{M}$	α	a	M	L_ν	$L_\nu/\dot{M}c^2$	$L_{\nu,ann}$	$L_{\nu,URCA}$	L_{photo}	L_{diss}	L_{ent}
0.01	0.1	0	3	0.015	8.6e-4	3.4e-3	0.012	0.200	0.859	0.644
0.01	0.01	0	3	0.650	0.036	0.012	0.638	0.200	0.724	-0.124
0.01	0.1	0.5	3	0.036	2.0e-3	9.9e-3	0.026	0.200	1.24	1.01
0.01	0.01	0	10	0.049	2.7e-3	9.3e-3	0.040	0.200	0.431	0.181
0.1	0.1	0	3	3.35	0.019	0.39	2.96	2.00	9.18	3.88
0.1	0.01	0	3	6.15	0.034	7.7e-3	6.14	2.00	7.44	-0.71
0.1	0.1	0.5	3	8.03	0.045	1.03	7.00	2.00	12.96	3.02
0.1	0.1	0.95	3	46.4	0.26	2.61	43.8	1.99	36.8	-11.5
0.1	0.1	0.95	6	26.2	0.15	7.24	19.0	2.00	31.1	3.20
1.0	0.1	0	3	86.3	0.048	0.66	85.7	19.9	90.9	-14.9
1.0	0.1	0.5	3	142.	0.078	1.53	140.	19.9	142.	-19.6
10.0	0.1	0	3	781.	0.043	53.3	728.	200.	836.	-135.
10.0	0.1	0.5	3	1285.	0.071	174.	1111.	200.	1263.	-211.

TABLE 3

Model				Values at horizon			
$\dot{M}$	α	a	M	ρ	T	ρV^2	N_{wind}
$M_\odot$ s^{-1}			$M_\odot$	10^{10} g cm^{-3}	10^{10} K	10^{30} erg cm^{-3}	
0.01	0.1	0	3	0.060	3.90	0.53	7.1
0.01	0.01	0	3	0.23	1.91	2.04	90.2
0.01	0.1	0.5	3	0.080	4.61	0.70	7.6
0.01	0.01	0	10	9.32e-3	1.96	0.083	19.7
0.1	0.1	0	3	0.69	6.46	6.14	9.6
0.1	0.01	0	3	2.10	2.04	18.8	87.9
0.1	0.1	0.5	3	1.07	7.42	9.45	10.2
0.1	0.1	0.95	3	12.0	5.83	98.7	14.0
0.1	0.1	0.95	6	0.88	9.04	7.46	10.2
1.0	0.1	0	3	12.6	5.71	113.	9.9
1.0	0.1	0.5	3	20.1	6.35	178.	11.5
10.0	0.1	0	3	86.6	11.4	774.	6.6
10.0	0.1	0.5	3	135.	13.1	1197.	7.4

TABLE 4

$\dot{M}$ ($M_\odot$ s^{-1})	α	a	M $M_\odot$	L_ν (10^{51} erg s^{-1})	$L_{\nu\bar{\nu}}$ (10^{51} erg s^{-1})	efficiency (%)
0.01	0.1	0	3	0.015	3.9×10^{-8}	0.0003
0.01	0.01	0	3	0.650	9.0×10^{-6}	0.001
0.01	0.1	0.5	3	0.036	5.9×10^{-7}	0.002
0.01	0.01	0	10	0.049	6.4×10^{-9}	10^{-5}
0.1	0.1	0	3	3.35	3.0×10^{-3}	0.09
0.1	0.01	0	3	6.15	8.0×10^{-4}	0.01
0.1	0.1	0.5	3	8.03	0.039	0.5
0.1	0.1	0.95	3	46.4	2.0	4.2
0.1	0.1	0.95	6	26.2	0.79	3.0
1.0	0.1	0	3	86.3	0.56	0.6
1.0	0.1	0.5	3	142	3.5	2.5
10.0[a]	0.1	0	3	(781)	(200)	(26)
10.0[a]	0.1	0.5	3	(1280)	(820)	(64)

[a] The assumption that the neutrinos are optically thin breaks down for accretion rates of 10 $M_\odot s^{-1}$ and above. The neutrino annihilation luminosities and energies listed for these high accretion simulations are upper limits.

TABLE 5

Model	Duration (s)	a	log $L_{\nu\bar{\nu}}$ (erg s^{-1})	log $E_{\nu\bar{\nu}}$ (erg)	Rate (Myr^{-1})[a]
n*+n*	0.1	0	50.7	49.7	0.1-5
		0.5	51.5	50.5	
n*+BH	0.1	0	(52)[b]	(51)[b]	0.1-50
		0.5	(52.6)[b]	(51.6)[b]	
Collapsar	10	0	48.5	49.5	$\lesssim$ 2000
		0.95	51.3	52.3	
BH+WD	15-150	0	43.6 - 47.7	46-49	0.1-50
		0.5	44.8 - 48.8	47-50	
BH+He core	15-500	0	43.6 - 48.5	46-50	1-1000
		0.5	44.8 - 49.6	47-51	

[a]This rate assumes a supernova rate of 0.02 yr^{-1}.
[b]Rough estimate owing to optically thick disk.

TABLE 6

Model[a]	Duration (s)	B_{15} (10^{15} gauss)	log L_{BZ} (erg s^{-1})	log E_{BZ} (erg)
n*+n*	0.1	10	51	50
n*+BH	0.1	10	51	50
Collapsar	10	1	49	51
BH+WD	15-150	1	49	50
BH+He core	15-500	0.3	48	51

[a]Assuming a=0.5 in all cases

Fig. 1.— A neutrino-cooled accretion disk solution (solid line) for an accretion rate $\dot{M} = 1$ M$_\odot$ s^{-1}, black hole spin $a = 0$, viscosity parameter $\alpha = 0.1$, and black hole mass $M = 3$ M$_\odot$. The six panels show the density ρ, temperature T, radial velocity V, disk height H, angular velocity Ω, and specific angular momentum l. Also shown for comparison purposes are a pure advection solution with no cooling (dotted line) and an analytic thin disk solution where URCA-process neutrino cooling balances viscous dissipation (dashed line).

Fig. 2.— Additional parameters for the solution shown in Fig. 1. Note that here the dashed and dotted lines have different meanings than in Fig. 1. The upper left panel shows the cooling rate due to neutrinos and photodisintegration (solid line), the heating rate due to viscous dissipation (dotted line), and the rate at which energy is added to the entropy of the gas (dashed line). The upper right panel shows $f = 1 - Q_{cool}/Q_{diss}$; the feature around $\log r = 6$ occurs because Q_{diss} briefly becomes negative here. The middle left panel shows the neutrino luminosity per unit radius. The middle right panel shows the cooling and accretion time scales. The two bottom panels show the pressure components: total pressure (solid), gas pressure (dotted), pressure due to radiation and pairs (short-dashed), and degeneracy pressure (long-dashed).

Fig. 3.— Solutions for four accretion rates: $\dot{M} = 0.01$ (short-dashed), 0.1 (solid), 1 (dotted), and 10 M$_\odot$ s^{-1} (long-dashed). All four have $a = 0$, $\alpha = 0.1$, and $M = 3$ M$_\odot$. The panels are as in Fig. 1, except for the two bottom panels which show the neutrino luminosity per unit radius and f.

Fig. 4.— Solutions for two values of the viscosity parameter $\alpha = 0.1$ (solid) and 0.01 (dashed). Both solutions have $\dot{M} = 0.1$ M$_\odot$ s^{-1}, $a = 0$, and $m = 3$ M$_\odot$.

Fig. 5.— Same as Fig. 4, except that here the two solutions have $\dot{M} = 0.01$ M$_\odot$ s^{-1}.

Fig. 6.— Solutions for three values of the black hole spin: $a = 0$ (solid), 0.5 (dashed), and 0.95 (dotted). All three solutions have $\dot{M} = 0.1$ M$_\odot$ s^{-1}, $\alpha = 0.1$, and $M = 3$ M$_\odot$.

Fig. 7.— Same as Fig. 3, except that here the four solutions all have $a = 0.5$.

Fig. 8.— The Kerr parameter a as a function of the fractional increase in the mass of a black hole accreting from a thin disk.

Fig. 9.— (a) Pair annihilation luminosity per cm versus radius for $\dot{M} = 0.1$ M$_\odot$ s^{-1} and $M_{\rm BH} = 3.0$ M$_\odot$. In addition, the total integrated luminosity out to each radius is plotted for the same models. These models are representative of the entire set, for all of which over half of the energy is injected in a narrow beam with equatorial radii $\lesssim 2 \times 10^6$ cm. (b) Pair annihilation luminosity per cm versus distance along the angular momentum axis. Again,

the total integrated luminosity out to each scale height above the plane is plotted for the same models.

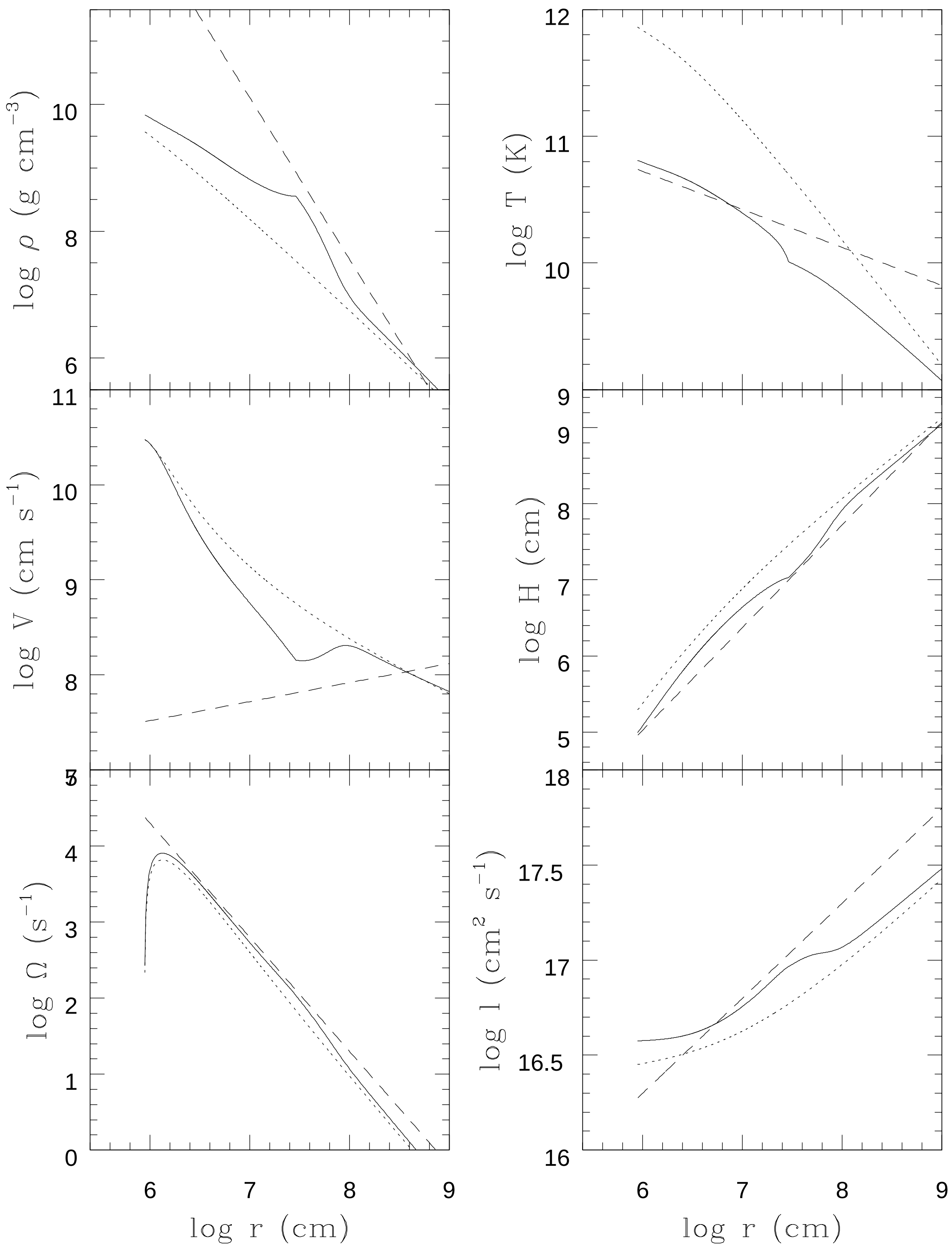

log ρ (g cm^{-3})
log T (K)
log V (cm s^{-1})
log H (cm)
log Ω (s^{-1})
log l (cm^2 s^{-1})
log r (cm)
log r (cm)

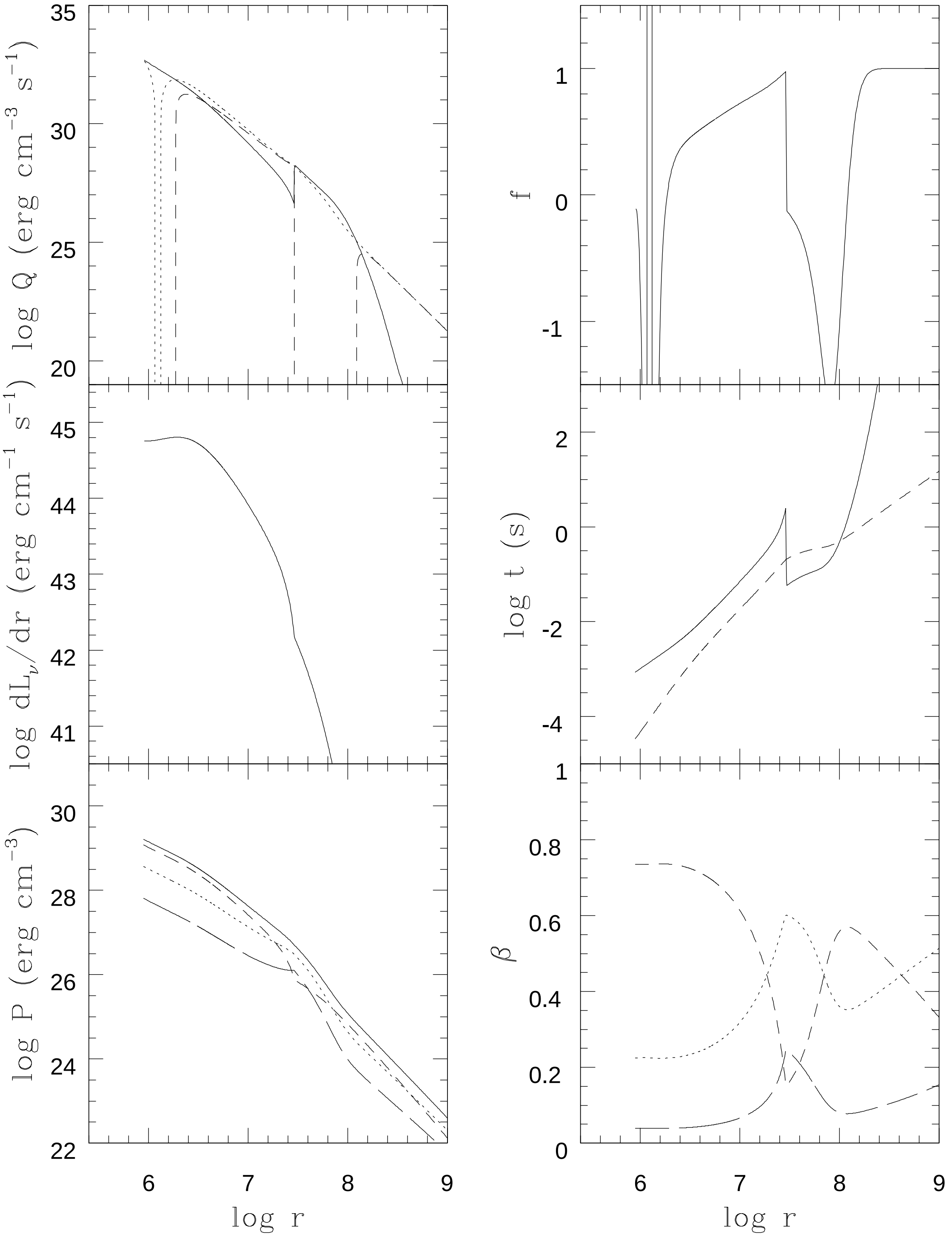

log Q (erg cm^-3 s^-1)
35
30
25
20
f
1
0
-1
log dL_ν/dr (erg cm^-1 s^-1)
45
44
43
42
41
log t (s)
2
0
-2
-4
log P (erg cm^-3)
30
28
26
24
22
β
1
0.8
0.6
0.4
0.2
0
6
7
8
9
log r
6
7
8
9
log r

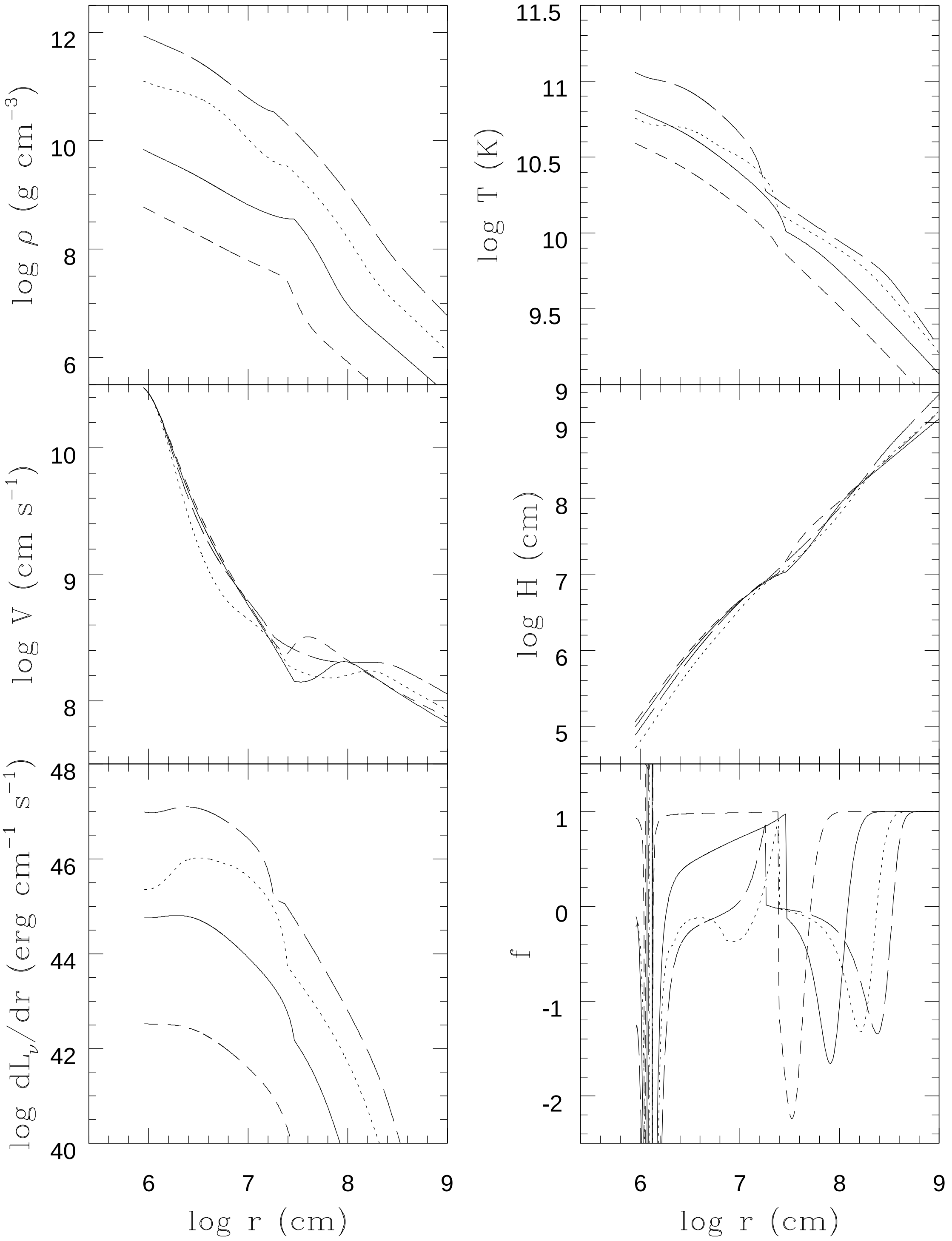

12
10
8
6
log ρ (g cm^{-3})
11.5
11
10.5
10
9.5
9
log T (K)
10
9
8
log V (cm s^{-1})
9
8
7
6
5
log H (cm)
48
46
44
42
40
log dL$_\nu$/dr (erg cm^{-1} s^{-1})
1
0
-1
-2
f
6
7
8
9
log r (cm)
6
7
8
9
log r (cm)

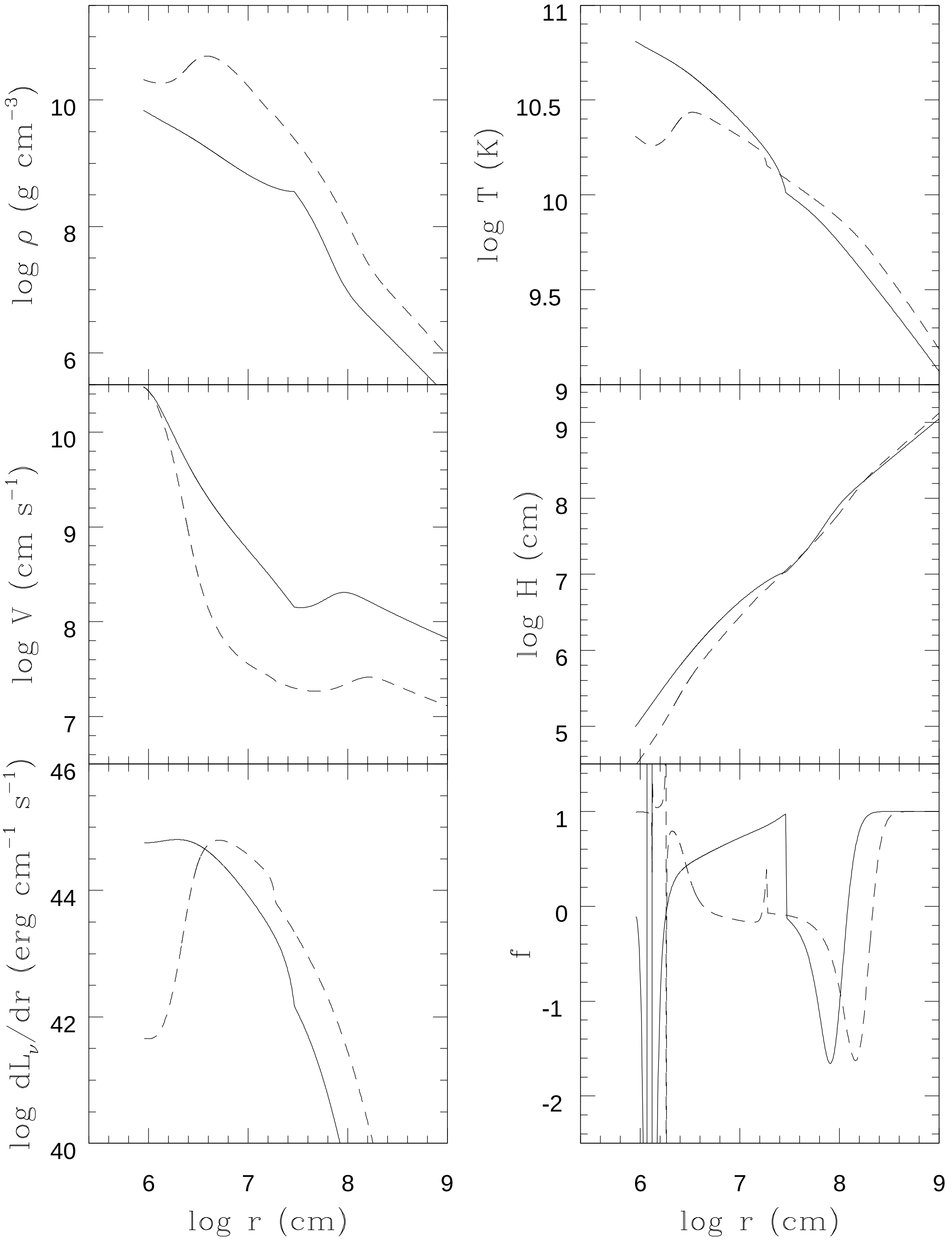
log ρ (g cm^{-3})
log T (K)
log V (cm s^{-1})
log H (cm)
log dL$_\nu$/dr (erg cm^{-1} s^{-1})
f
log r (cm)
log r (cm)

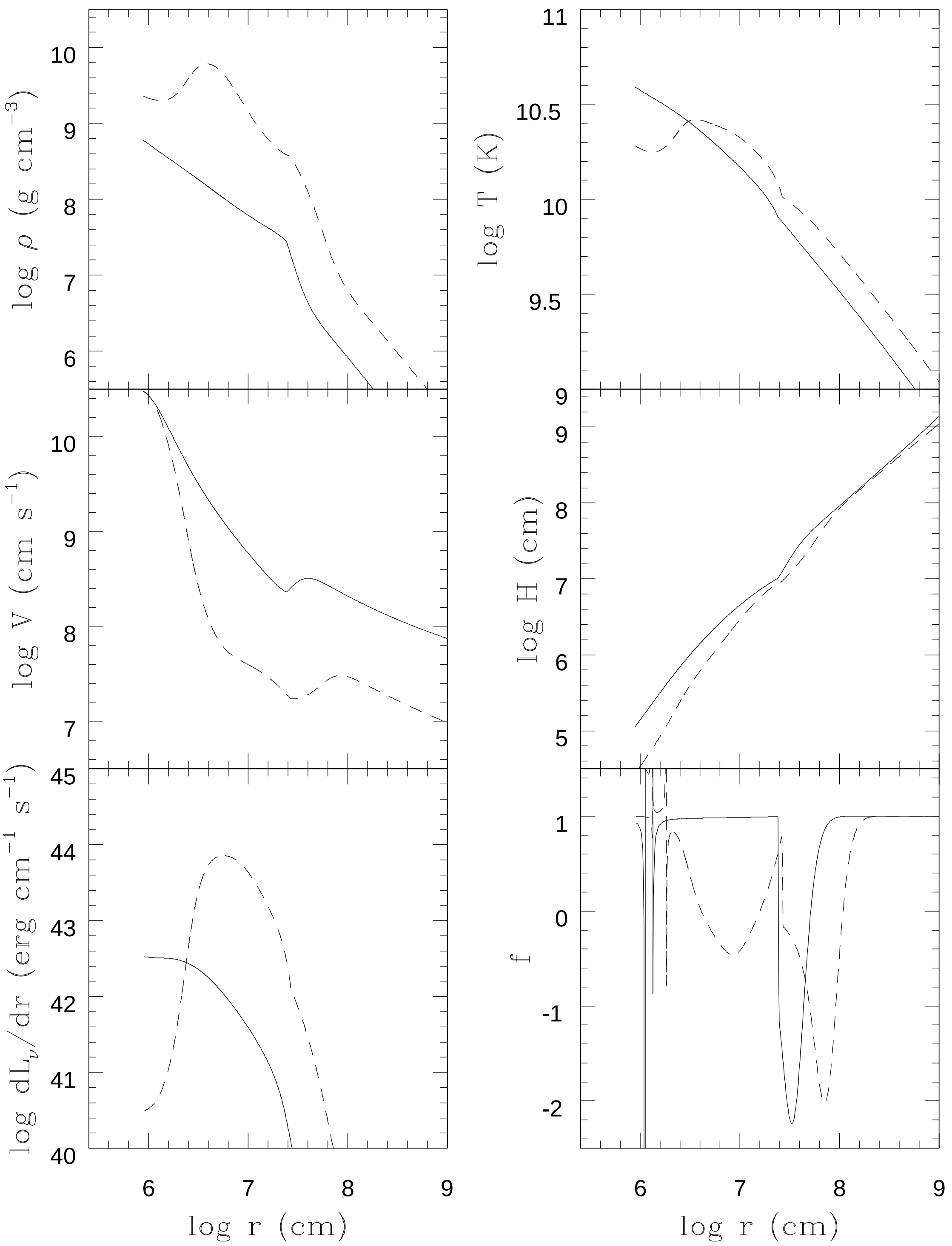
log ρ (g cm^{-3})
10
9
8
7
6
log T (K)
11
10.5
10
9.5
9
log V (cm s^{-1})
10
9
8
7
log H (cm)
9
8
7
6
5
log dL$_\nu$/dr (erg cm^{-1} s^{-1})
45
44
43
42
41
40
f
1
0
-1
-2
6
7
8
9
log r (cm)
6
7
8
9
log r (cm)

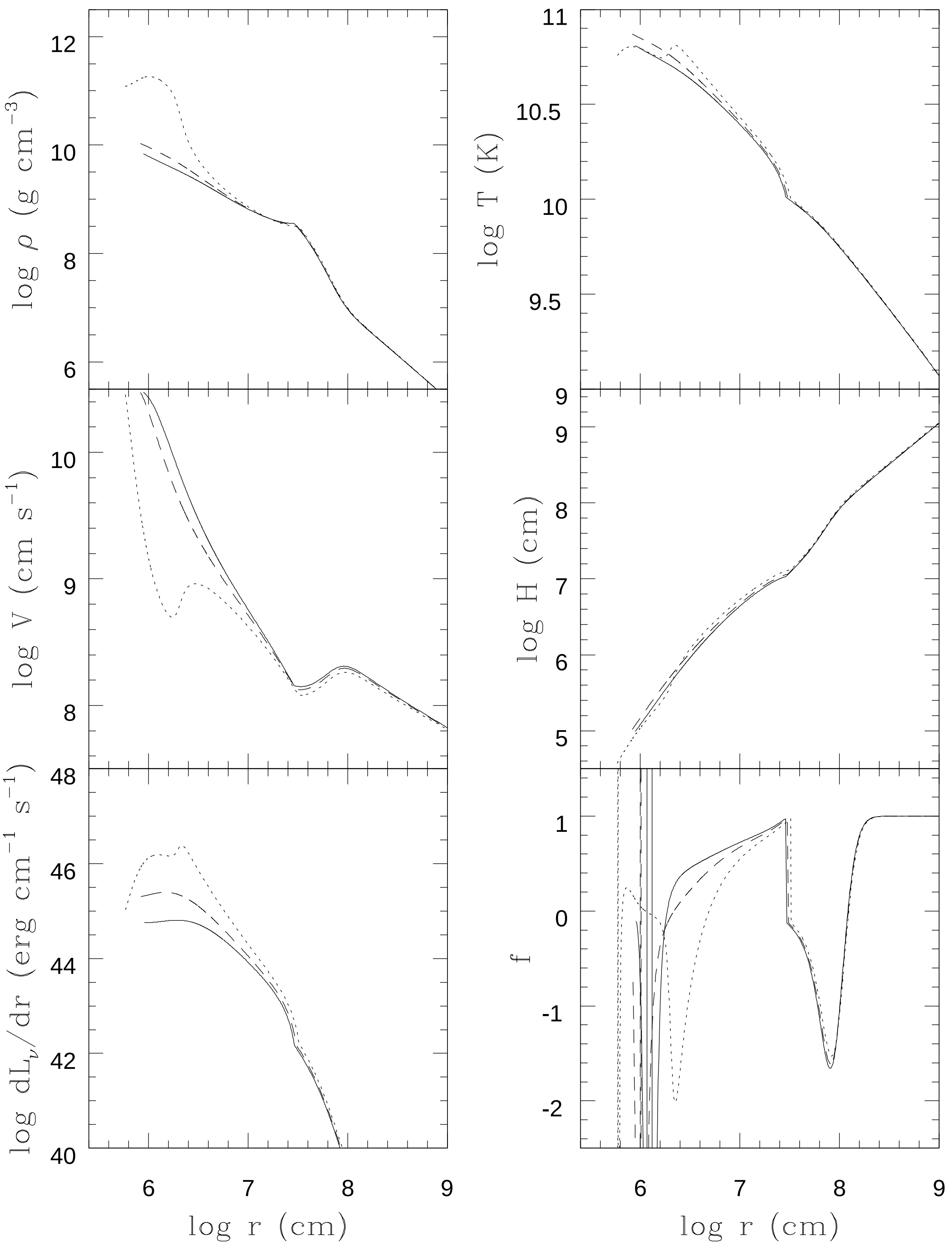
log ρ (g cm^{-3})
log T (K)
log V (cm s^{-1})
log H (cm)
log dL$_\nu$/dr (erg cm^{-1} s^{-1})
f
log r (cm)
log r (cm)

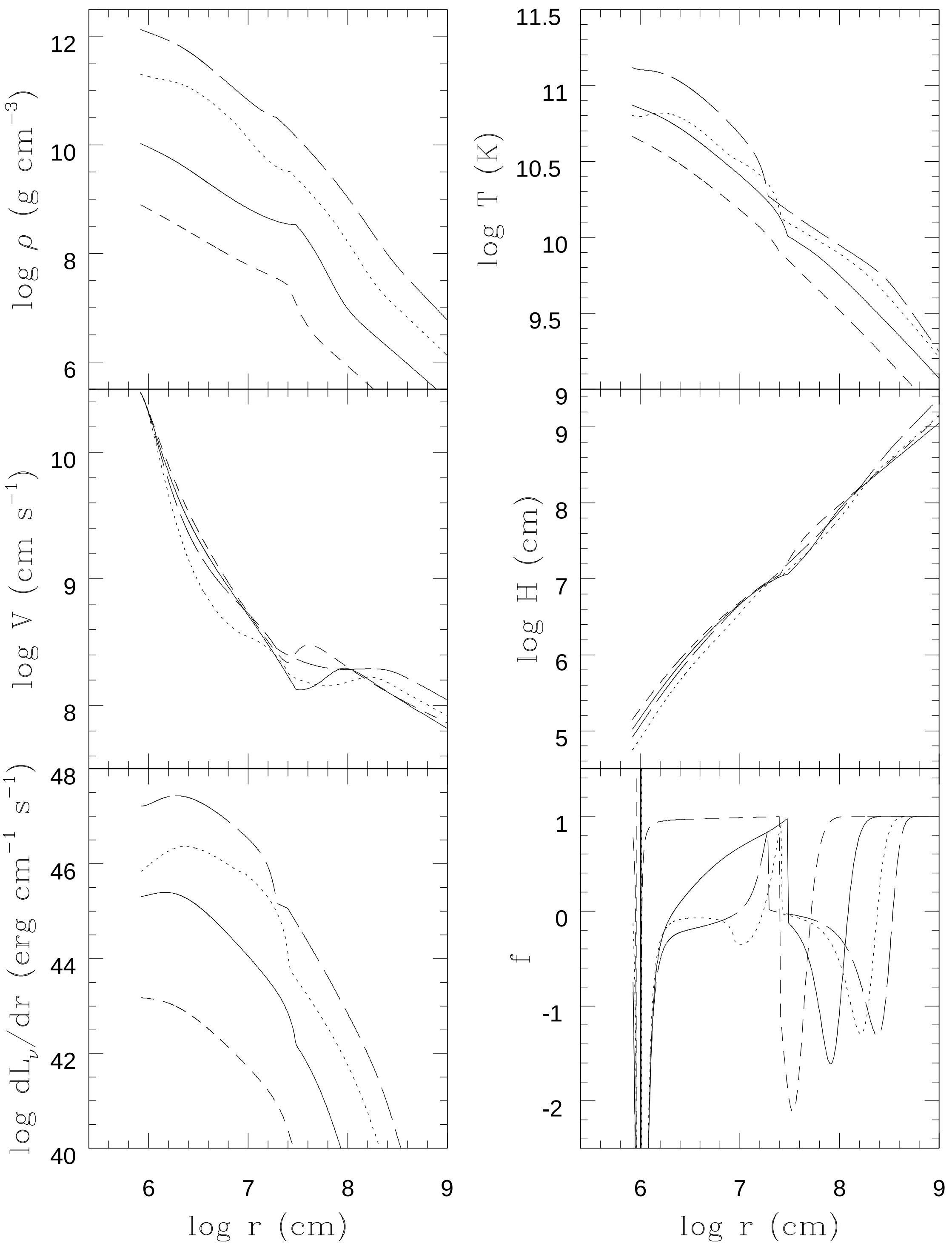
log ρ (g cm^-3)
log T (K)
log V (cm s^-1)
log H (cm)
log dL_ν/dr (erg cm^-1 s^-1)
f
log r (cm)
log r (cm)

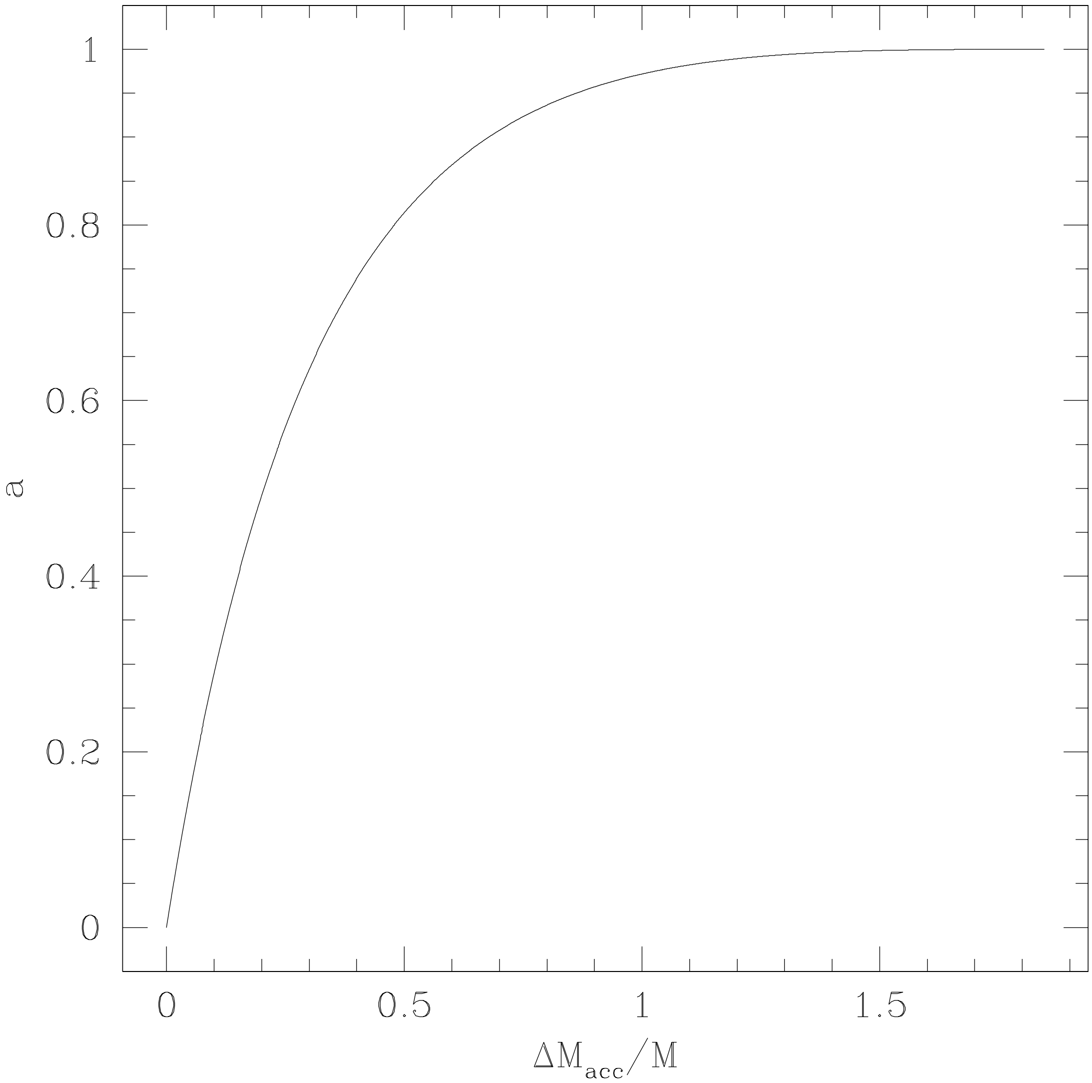

a
0
0.2
0.4
0.6
0.8
1
0
0.5
1
1.5
ΔM_acc/M

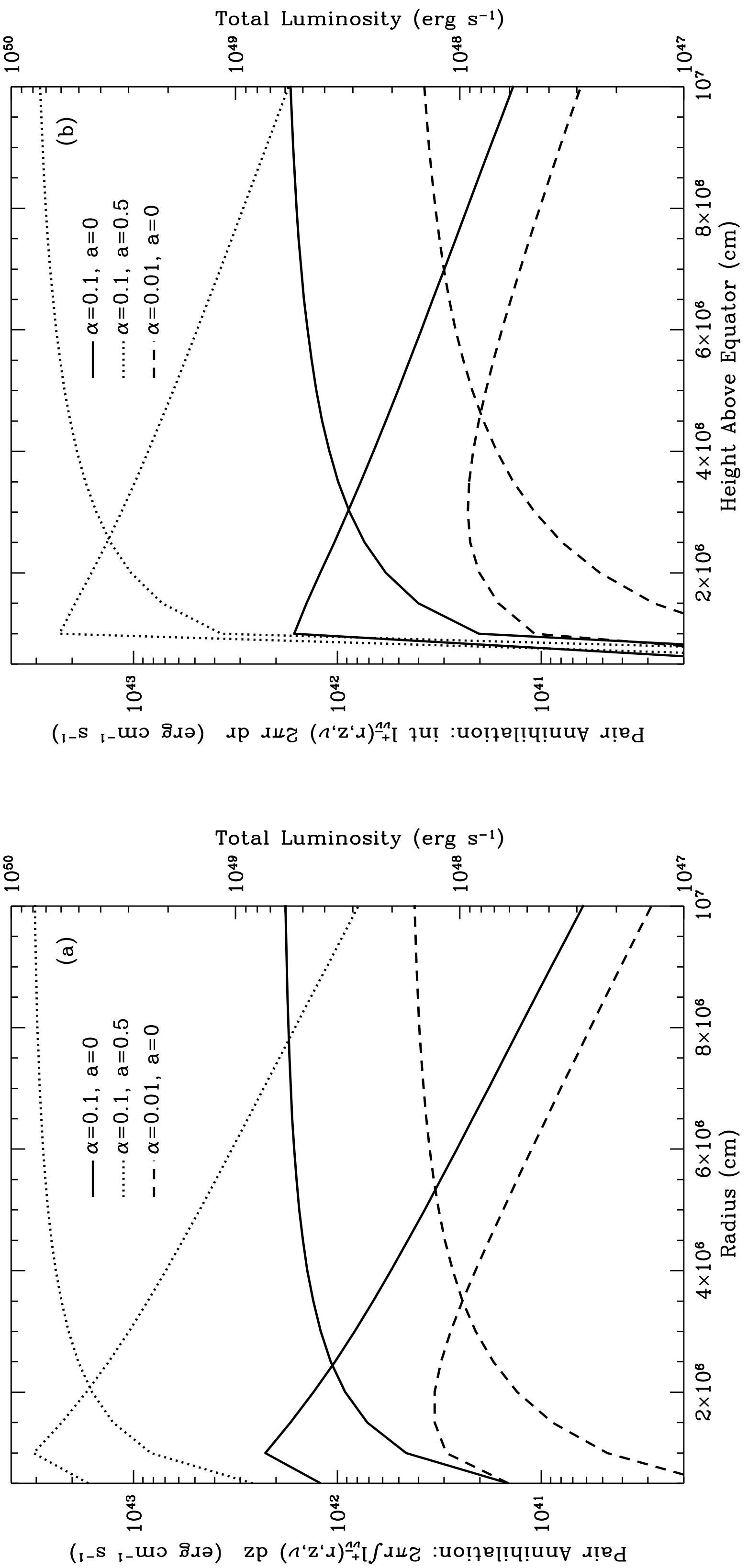
(b)
α=0.1, a=0
α=0.1, a=0.5
α=0.01, a=0
Total Luminosity (erg s⁻¹)
Height Above Equator (cm)
Pair Annihilation: int $l_+^{\nu\bar{\nu}}(r,z,\nu)$ 2πr dr (erg cm⁻¹ s⁻¹)
(a)
α=0.1, a=0
α=0.1, a=0.5
α=0.01, a=0
Total Luminosity (erg s⁻¹)
Radius (cm)
Pair Annihilation: $2\pi r \int l_+^{\nu\bar{\nu}}(r,z,\nu)$ dz (erg cm⁻¹ s⁻¹)